examinations. They were housed in vinyl isolators with sterilized Clean tip (CLEA Japan, Inc., Tokyo) as bedding and given sterilized water and sterilized commercial CL-2 pellets (CLEA Japan, Inc.) ad libitum. The diet was sterilized with an autoclave (121°C, 30 min). Five male and five female mice were inoculated at 4 weeks of age into the stomach by a metal catheter with 0.5 ml of a 10^{-1} suspension of feces obtained from an apparently healthy human volunteer (male, aged 59 years). The mice were mated at 8 weeks of age, and their offspring were weaned at 3 weeks of age.

Sampling. Fecal samples from mice were taken 1, 2, and 4 weeks after administration of the fecal suspension. Eight weeks after inoculation, the mice were sacrificed by use of diethyl ether, and the contents of the small intestine, cecum, and colon were removed as samples of the intestinal microbial community. Collected samples were stored immediately at −80°C until use. Intestinal content samples from the offspring were collected at 6 weeks of age by the same methods.

Cell lysis and DNA isolation from samples. DNA extraction and purification were based on the methods described by Clement and Kitts (3), using an Ultra Clean Soil DNA isolation kit (Mo Bio Laboratories, Inc., Solana Beach, CA) with some modification, as described previously (17).

T-RFLP analysis. A pair of universal primers, 5′ FAM (6-carboxyfluorescein)-labeled 27f (5′-AGAGTTTGATCCTGGCTCAG-3′) (Applied Biosystems, Tokyo, Japan) and 1492r (5′-GGTTACCTTGTTACGACTT-3′) (18), were used. PCR was performed as described previously (17). Purified PCR products were digested with 20 U of HhaI (Takara Bio Inc.) in a total volume of 10 μl at 37°C for 3 h. The lengths of the terminal restriction fragments (T-RFs) were determined using standard size markers GS500 ROX and GS 1000 ROX (Applied Biosystems) with an ABI PRISM 310 genetic analyzer (Applied Biosystems) and GeneScan analysis software (Applied Biosystems). Cluster analysis was performed using BioNumerics software (Applied Maths, Sint-Martens-Latem, Belgium) based on T-RFLP patterns. The Jaccard matching coefficient was used for objective interpretation of the difference in T-RF patterns. The distances of similarity among samples were represented graphically by constructing a dendrogram. The unweighted pair-group method with arithmetic mean (UPGMA) was used to establish the dendrogram type. T-RFs were quantified as the proportion of total peak area of all T-RFs. The significant differences between the samples at 1 week after administration and other time points were calculated using Student's t test ($P < 0.05$). Characteristic peaks were identified by direct cloning of T-RFs as previously described (22). Reproducibility of T-RFLP patterns was previously investigated in detail (25, 34).

16S rRNA gene sequences. The human inoculum, mouse fecal samples 1 and 4 weeks after administration, and mouse colon samples 8 weeks after administration were used for cloning and sequencing to compare with T-RFLP analysis results. Sequencing of the 16S rRNA genes was performed based on a previous study (17). All sequences were compared with similar sequences of the reference organisms by BLAST (1) and FASTA (27) searches and checked for possible chimeric artefacts by the CHIMERA CHECK program of the Ribosomal Database Project-II (4). All sequences underwent fragment analysis with restriction enzymes by computer simulation and were compared by T-RFLP analysis. The term "phylotype" is used for a cluster of clone sequences that differs from the sequence of a known species by approximately 2%, and these clusters were at least 98% similar to numbers within a cluster of clone sequences (26).

PCR and sequencing for the detection of HDL. Three primer sets were used for the detection of HDL. One primer and one primer set used in this study were designed in previous studies of the detection of lactic acid bacteria (LAB) or *Lactobacillus* spp. (11, 40). A reverse primer; S-G-Lab-0677-a-A-17 (Lab-0677r, 5′-CACCGCTACACATGGAG-3′), was designed by Heilig et al. (11). Two primers, Lac 1 (5′-AGCAGTAGGGAATCTTCCA-3′) and Lac 2 (5′-CATGT GTAGCGGTGRAAT-3′), were designed by Walter et al. (40). Lab-0677r was used with 5′ FAM-labeled 27f for LAB-specific T-RFLP analysis of the human inoculum and intestinal contents of HFA mice. LAB-specific T-RFLP analysis was performed with four restriction enzymes, HhaI, MspI, HaeIII, and AluI. The 27f–Lab-0677r primer set and Lac 1-Lac 2 primer set were also used in cloning to identify amplicons. The amplification program conformed to the description of each previous study (11, 40). After the identification of HDL, we designed the forward primer HDL-f (5′-AGGATAGAGGC-3′) to amplify the HDL. Nested PCR was performed to detect the HDL. Lac 1 and Lac 2 were used for first-round PCR. HDL-f and Lac 2 were used for second-round PCR. The program included 94°C for 3 min; 30 cycles consisting of 94°C for 30 s, 51°C for 30 s, and 72°C for 30 s; and a final extension period at 72°C for 3 min. Ten nanograms of DNA from the first-round PCR amplicon was subjected to a second PCR in a 50-μl reaction mixture. Amplified DNA was verified by 1.5% agarose gel electrophoresis and sequencing.

Nucleotide sequence accession numbers. Sequences of the 16S rRNA genes of new phylotypes derived from humans in this study were deposited with the GenBank database under accession numbers AB191009 to AB191022. Representative sequences of the 16S rRNA genes confirmed in this study, i.e., of HDL derived from human inoculum, of an *Aerococcus* sp. derived from HFA mouse intestine, and of HDL derived from HFA mouse intestine, were deposited in GenBank under accession numbers AB191025 to AB191027, AB191028 to AB191030, and AB191023 to AB191024, respectively.

RESULTS

Dynamics of intestinal microbiota in HFA mice. The shift of intestinal microbiota in HFA mice after the administration of human feces was determined by T-RFLP patterns. Unique changes over time were revealed by T-RFLP profiles of samples derived from HFA mice (Fig. 1). Common or characteristic T-RFs were detected in all samples. Characteristic T-RFs detected in all samples were confirmed numerically, and significance was calculated by Student's t test ($P < 0.05$) (Table 1). Increases in T-RFs over time were at bp 56, 184, and 196; in contrast, decreases in T-RFs with time were at bp 366. Although the T-RFs at bp 730 were detected at a high rate in human inoculum, they were not detected at such a high rate in HFA mouse samples. T-RFs at bp 231, 440, and 808 were detected in samples of intestinal contents but were not detected or were detected in small populations in fecal samples. We designated these T-RFs as "persisting." 16S rRNA gene clone library analysis and direct cloning of T-RFs were used to identify these unique movements (Table 1). All sequences obtained from each sample had a fragment position confirmed by computer simulation. Almost all the T-RFs were presumed to represent species or phylotypes detected by 16S rRNA gene clone library analysis. The same identification was confirmed by direct cloning of T-RFs (data not shown).

16S rRNA gene sequencing of intestinal microbiota in the human inoculum and HFA mice. The numbers of clones detected in samples of the inoculum, in a fecal sample 1 and 4 weeks after administration, and in a colon sample 8 weeks after administration are shown in Table 2. One hundred eighty-seven clones from the inoculum were analyzed. Sequences were classified into 12 phylogenetic groups. Although no exact 16S rRNA gene similarity limits exist to define specific taxa such as genus and species, species definition in general requires sequence similarities of greater than 98% (36). All clones were divided into 81 species, including phylotype. About 83% of clones detected in samples of the inoculum belonged to phylotypes. About 40 clones derived from fecal samples at 1- and 4-week time points were analyzed because the T-RFLP patterns at these two time points in HFA mice resembled each other. Additionally, about 40 clones derived from the colon sample at 8 weeks in HFA mice were analyzed. Clones identified as the *Bacteroides* group, the *Clostridium* cluster IV, or the *Clostridium* cluster XIVa were detected at a high rate in all samples, including the human inoculum. Clones belonging to the "*Gammaproteobacteria*" group, the *Verrucomicrobium* group, and the *Coriobacteriaceae* were detected only in samples from HFA mice.

Cluster analysis of intestinal microbiota in the offspring of HFA mice. We performed dendrogram analysis based on Jaccard matching coefficients of T-RFLP profiles to assess the similarity of microdiversity in the intestine among the samples. UPGMA was used for the dendrogram (Fig. 2). The human inoculum was compared with other human fecal samples (Fig.

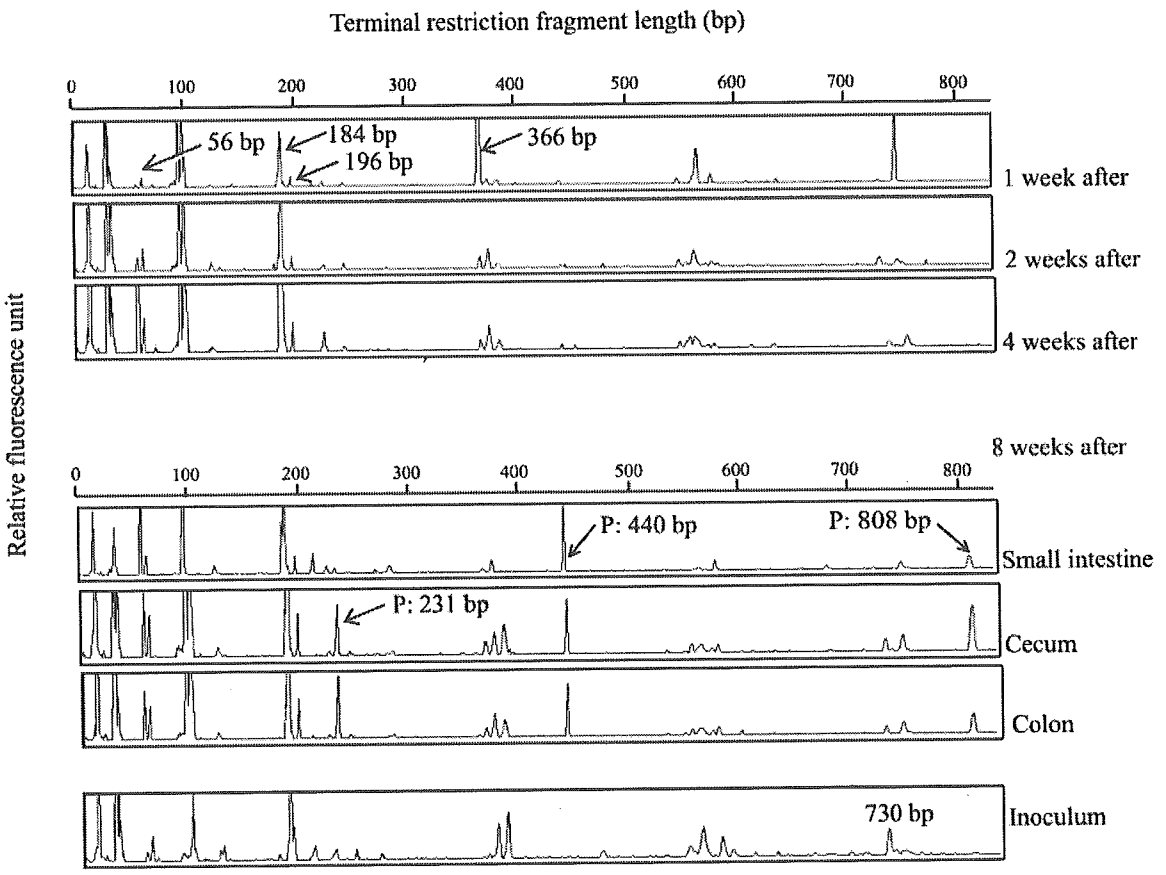

FIG. 1. Movement of intestinal microbiota in HFA mice by T-RFLP analysis. T-RFLP patterns of 16S rRNA genes from samples digested with HhaI. The minimum and maximum values of the ordinate are 0 to 500 fluorescence units. The unique T-RFs are shown by arrows. The peaks detected in only the intestinal contents of HFA mice are indicated as persisting (P).

2A). The difference in similarity indices among the samples, except for the Hu-2 sample, was not significant by *t* test. In addition, T-RFLP patterns of samples from HFA mice and their offspring were determined in addition to those of human samples (Fig. 2B). The dendrogram was divided into two clusters (I and II). Cluster I was formed by only human samples, excluding the human inoculum. Cluster II was formed by samples from HFA mice and their offspring and the human inoculum. Moreover, for similarity indices of about 45%, cluster II was divided into two subclusters (II-α and II-β). The inoculum sample became an outgroup of cluster II. Subcluster II-α was composed only of samples from HFA mice, and subcluster II-β was composed only of samples from offspring.

Detection of HDL by specific primers. To confirm the existence of HDL in the intestine of HFA mice, three primer sets were used in this study. The first set, primer 27f and the Lab-0677r primer designed by Heilig et al. (11), was used for LAB-specific T-RFLP analysis with four restriction enzymes (HhaI, MspI, HaeIII, and AluI). T-RFs derived from HFA mouse samples by use of this primer set appeared at bp 588 to 589, 556 to 560, 263 to 264, and 683 to 684, digested by HhaI, MspI, HaeIII, and AluI, respectively.

From the computer simulation results, any bacteria belonging to the genus *Lactobacillus* were not assigned to these restriction sites. On the other hand, T-RFs derived from the human inoculum appeared at bp 691 (digested by HhaI), at bp 134 and 164 (digested by MspI), at bp 213 (digested by HaeIII), and at bp 68 and 246 (digested by AluI). The T-RFLP analysis results were different for the inoculum and HFA samples. However, these restriction sites were also not assigned. To identify the composition of bacteria in these T-RFs, amplicons from HFA mouse samples were confirmed by cloning and sequencing. All clones derived from HFA samples were more than 98% similar to the species *Aerococcus viridans* at *Escherichia coli* positions 27 to 677. The restriction fragment lengths of the *Aerococcus viridans* clones were 581, 555, 266, and 1,069 bp, digested by HhaI, MspI, HaeIII, and AluI, respectively. There was no restriction site for AluI at positions 27 to 677. This result was identical with LAB-specific T-RFLP results for HFA mouse samples. We found no lactobacilli in HFA samples by use of the 27f–Lab-0677r primer set. Therefore, another primer set, Lac 1-Lac 2, was used. This primer set was designed by Walter et al. (40) for the amplification of LAB from samples. These amplicons were confirmed by cloning and sequencing. Clones derived from the human inoculum were more than 98% similar to the species *Lactobacillus delbrueckii* at *Escherichia coli* positions 355 to 644. These clones were designated HDL. However, clones derived from HFA mice

TABLE 1. Dynamics and persistence of characteristic T-RFs and identification of the T-RFs

Position (bp)	Ratio of T-RF area at indicated time after administration[a]						Trend[b]	Ratio of T-RF area in inoculum feces	Identification by 16S clone libraries
	Feces			Small intestine	Cecum	Colon			
	1 wk	2 wk	4 wk						
56	0.17 ± 0.02	0.63 ± 0.08*	2.72 ± 0.89*	3.91 ± 1.09*	1.50 ± 0.31*	1.23 ± 0.34*	↑	0.32 ± 0.02	ND[c]
184	0.41 ± 0.07	0.70 ± 0.06*	3.87 ± 1.81*	3.24 ± 0.64*	1.82 ± 0.58*	1.84 ± 0.98	↑	0.84 ± 0.10	Uncultured *Clostridium* cluster XVIa
196	0.60 ± 0.06	0.66 ± 0.06	0.91 ± 0.06*	1.16 ± 0.17*	0.89 ± 0.20	1.09 ± 0.27	↑	ND	Uncultured *Clostridium* cluster XVIa
231	ND	ND	0.20	14.3 ± 11.6	1.29 ± 0.36	1.79 ± 0.75	P	ND	Uncultured *Clostridium* cluster VI
366	20.7 ± 5.37	1.03 ± 0.08*	1.07 ± 0.37*	1.45 ± 0.60*	1.08 ± 0.32*	0.85 ± 0.16*	↓	0.64 ± 0.13	"*Gammaproteobacteria*" and *Coriobacteriaceae*
440	0.31 ± 0.01	0.32 ± 0.05	0.24 ± 0.01*	6.25 ± 1.17*	2.62 ± 0.21*	2.52 ± 0.54*	P	ND	Uncultured firmicutes
730	0.33 ± 0.05	0.85 ± 0.17	0.52 ± 0.09	ND	0.91 ± 0.15*	0.61 ± 0.17		1.37 ± 0.26	Uncultured *Clostridium* clusters VI and IX
808	ND	ND	ND	2.88 ± 1.25	1.59 ± 0.30	1.24 ± 0.32	P	ND	ND

[a] Values are ratios of a characteristic T-RF area to total area (mean ± standard error). Values for small intestine, cecum, and colon were determined at 8 weeks. *, Significantly different by paired *t* test from the value for the sample at 1 week.
[b] Changes in T-RF area after administration of human inoculum over time. ↑, increase; ↓, decrease; P, persistent in intestine.
[c] ND, not detected as T-RFs or clones.

were not similar to HDL but were similar to *Aerococcus* spp. This result was identical to the result determined with another primer set (27f–Lab-0677r). Therefore, in the second PCR, a primer (HDL-f) was designed to discriminate between HDL and other LAB. HDL were detected in seven of all the samples from HFA mice (Table 3). All amplified products were confirmed by sequencing.

DISCUSSION

Horizontal transmission of intestinal microbiota in HFA mice. HFA mice have been exploited and used as a tool reflecting human intestinal microbial ecology (6, 7, 30). Although the development of intestinal microbiota in HFA mice has been revealed by culture methods (12), there are few reports of the use of molecular methods (5, 7, 15). Our work has revealed the movement and persistence of human intestinal microbiota in formerly germfree mice by T-RFLP analysis. Additionally, some bacteria in unique T-RFs were identified in a comparison with 16S rRNA gene sequences and direct cloning of T-RFs (Table 1). Only a proportion of the T-RF peak at bp 366, identified as the "*Gammmaproteobacteria*" group and/or *Coriobacteriaceae*, was reduced. We also confirmed that the increased T-RFs were affiliated with the *Clostridium* group. According to the culture method (12), the number of *Enterobacteriaceae* decreased rapidly after the third day after inoculation. Conversely, anaerobic bacteria were dominant in HFA mice. Our results are in agreement with previous studies (12) because the "*Gammmaproteobacteria*" group belonging to *Enterobacteriaceae* and bacteria of the *Clostridium* group are anaerobic bacteria. However, most of the bacteria isolated in this study belonged to phylotypes. Briefly, most of human intestinal bacteria with unique shifts in the intestines of HFA mice have not yet been cultured.

HFA mice have limitations as a model because some of their enzyme activities and products of intestinal microbiota are different from those of humans. This result indicates that the limitations of HFA mice are caused by the differential composition of bacteria belonging to phylotypes. Bacteria in the *Clostridium* cluster XIVa and the *Clostridium* cluster IV were dominant in specific-pathogen-free mice and in conventional mice (9, 16, 17, 29). In spite of different environments, *Clostridium* group bacteria can inhabit the mouse intestine. Therefore, the physiological conditions of the mouse intestine might be suitable for these bacteria.

The change of indigenous bacteria in the intestine. The 16S rRNA gene clone sequences were used to identify microbiota of the human inoculum and of samples from HFA mice (Table 2). Clones belonging to the *Bacteroides* group, the *Clostridium* cluster IV, and the *Clostridium* cluster XIVa were detected in all samples at a high rate. However, clones belonging to the "*Gammmaproteobacteria*" group, the *Verrucomicrobium* group, the "*Deltaproteobacteria*" group, and the *Coriobacteriaceae* were detected only in samples from HFA mice. Godon et al. (8) reported the relationship between the number of sequences and the cumulative number of operational taxonomic units. In this study, despite the analysis of a small number of clones, many clones of these bacteria were detected only in HFA mice. This indicated the possibility that the population of these bac-

TABLE 2. Numbers of species and clones detected in 16S rRNA sequences

Bacterial group	Human sequences				HFA mouse sequences											
					1 wk[a]				4 wk				8 wk			
	No.		Ratio (%)		No.		Ratio (%)		No.		Ratio (%)		No.		Ratio (%)	
	s/p[b]	Clone	s/p	Clone	s/p	Clone	s/p	Clone	s/p	Clone	s/p	Clone	s/p	Clone	s/p	Clone
Bacteroides	11	19	13.6	10.4	6	7	37.5	25.9	4	4	50.0	30.8	5	16	23.8	38.1
Clostridium cluster I	2	3	2.5	1.6	ND[c]	ND			ND	ND			ND	ND		
Clostridium cluster IV	23	54	28.4	29.5	3	4	18.8	14.8	1	4	12.5	30.8	3	3	14.3	7.1
Clostridium cluster IX	6	14	7.4	7.7	ND	ND			ND	ND			ND	ND		
Clostridium cluster XIVa	29	53	35.8	29.0	6	8	37.5	29.6	2	2	25.0	15.4	7	7	33.3	16.7
Clostridium cluster XIVb	1	2	1.2	1.1	ND	ND			ND	ND			ND	ND		
Clostridium cluster XVI	1	24	1.2	13.1	ND	ND			ND	ND			ND	ND		
Clostridium cluster XVIII	1	1	1.2	0.5	ND	ND			ND	ND			ND	ND		
Unclass *Clostridium*	3	7	3.7	3.8	ND	ND			ND	ND			ND	ND		
Streptococcus	2	3	2.5	1.6	ND	ND			ND	ND			ND	ND		
Actinobacteria	1	2	1.2	1.1	ND	ND			ND	ND			ND	ND		
"*Deltaproteobacteria*"	1	1	1.2	0.5	ND	ND			ND	ND			1	1	4.8	2.4
"*Gammaproteobacteria*"	ND	ND			1	8	6.3	29.6	ND	ND			ND	ND		
Verrucomicrobium	ND	ND			ND	ND			1	3	12.5	23.1	4	14	19.0	33.3
Coriobacteriaceae	ND	ND			ND	ND			ND	ND			1	1	4.8	2.4
Total	81	183	100	100	16	27	100	100	8	13	100	100	21	42	100	100

[a] The time point after administration.
[b] s/p, species or phylotype.
[c] ND, not detected as clones.

teria was changed between the intestines of humans and HFA mice.

Almost all T-RFs of bacteria in the *Bacteroides* group in the database, which were digested with HhaI, are located from bp 94 to 104. Moreover, the computer simulation confirmed that clones in the *Verrucomicrobium* group corresponded to T-RFs at bp 98 with HhaI digestion. Therefore, T-RFs of both groups overlapped at bp 98. Although the movement of the T-RFLP pattern at bp 98 was not confirmed, the dominant bacterial group in HFA mice might change from those present in inoculated human feces.

Movement of intestinal microbiota to the offspring of HFA mice. By the use of culture methods, an earlier study revealed that HFA mice could be reproduced by breeding (14). In the present study, T-RFLP analysis was used to confirm the transfer of intestinal microbiota to the offspring of HFA mice. To compare the whole T-RFs in samples, we used dendrogram analysis derived from the similarity of T-RFLP patterns among samples. The human inoculum was compared with other human fecal samples (Fig. 2A). The inoculum sample was not specific among human fecal samples because it was not an outgroup of the cluster. This result was confirmed by a *t* test of similarity indices among T-RFLP patterns. T-RFLP patterns of samples from HFA mice and their offspring were determined in addition to those from human samples (Fig. 2B). The dendrogram was divided into two large clusters. Cluster I was composed only of human samples. Cluster II was composed of samples from HFA mice, their offspring, and the human inoculum. This result indicated that the intestinal microbiota of HFA mice and their offspring was more similar to that of the inoculum than to that of other human samples. Moreover, this result indicated that the composition of intestinal microbiota of HFA mice and their offspring reflected the individual differences of human intestinal microbiota. On the other hand, cluster II was divided into two subclusters. Subcluster II-α was composed of samples from HFA mice, and subcluster II-β was composed only of samples from the offspring. These results indicated that the microbiota in HFA mice was changed by host-specific modification from the bacterial composition of the inoculum in their intestines, although the intestinal microbiota of HFA mice and their offspring reflected the composition of the inoculum as in previous studies (14). Moreover, the intestinal microbiota of offspring showed greater modifications than did the microbiota of their parents.

Existence of the HDL in HFA mice. The genera *Lactobacillus* and *Bifidobacterium* derived from humans seem to hardly colonize in the mouse intestine (13, 28, 41). In particular, although lactobacilli are the predominant bacteria in the mouse intestine, previous studies could not detect them in HFA mice (13, 28) by culture methods. We used three primer sets in this study (27f–Lab-0677r, Lac 1-Lac 2, and HDL-f–Lac 2). Two LAB-specific primer sets (27f–Lab-0677r and Lac 1-Lac 2) were used to detect LAB in the human inoculum and in the HFA mouse intestine. HDL was detected in the human inoculum by LAB-specific primer sets. However, clones detected from the HFA mouse intestine were identified not as HDL but as bacteria of the genus *Aerococcus* by both primer sets. The clone identified as the *Aerococcus* species was not detected in the human inoculum. From the results of the differential detection, our results suggested that the populations of HDL and *Aerococcus* bacteria in samples were different between the human inoculum and the HFA mouse intestine. Therefore, a specific primer for HDL was designed to detect HDL in the intestines of HFA mice, and we performed nested PCR for increased sensitivity of detection. Consequently, HDL were detected in seven samples from HFA mice (Table 3) and

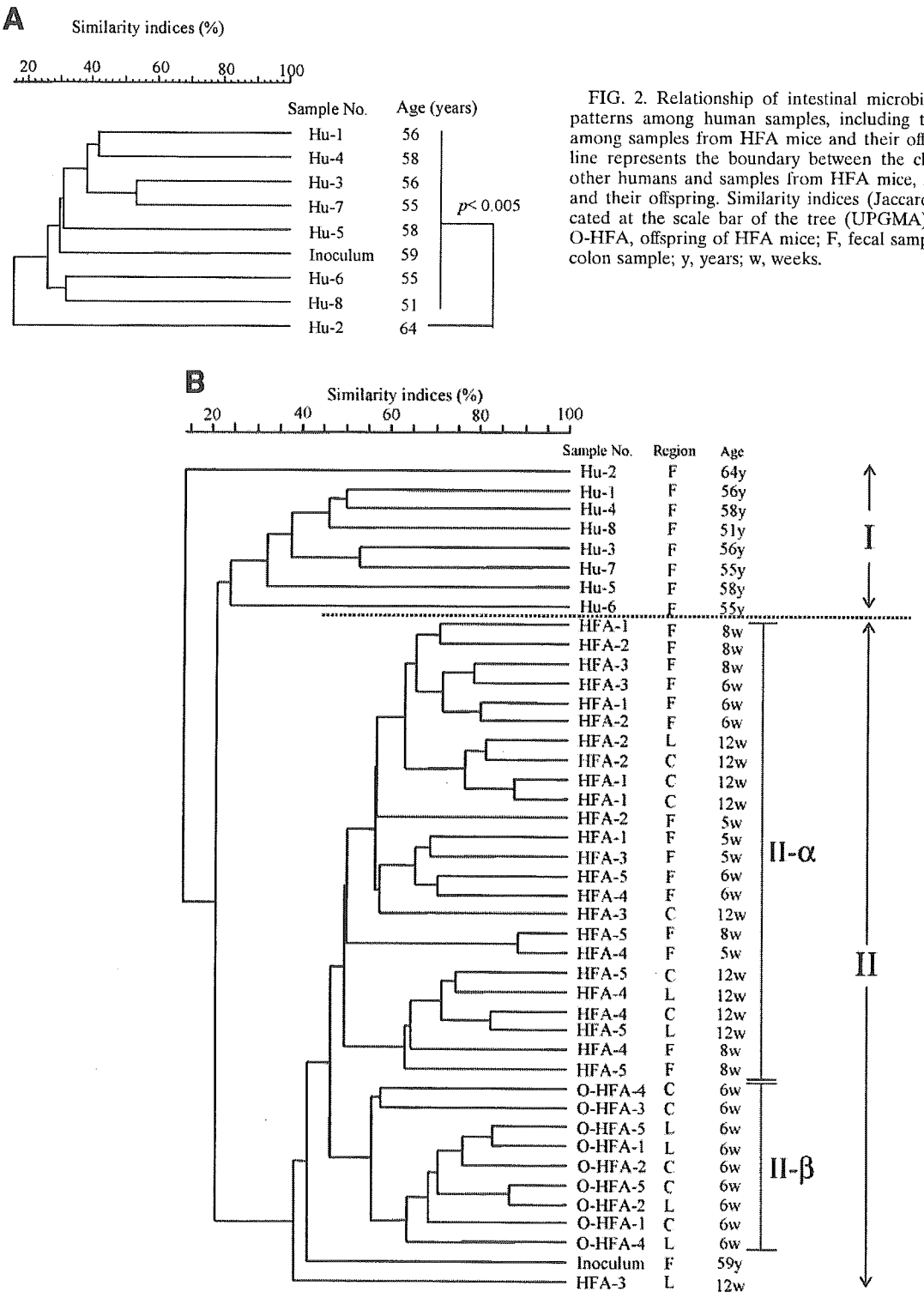

FIG. 2. Relationship of intestinal microbiota based on T-RFLP patterns among human samples, including the inoculum (A), and among samples from HFA mice and their offspring (B). The dotted line represents the boundary between the cluster of samples from other humans and samples from HFA mice, including the inoculum and their offspring. Similarity indices (Jaccard coefficients) are indicated at the scale bar of the tree (UPGMA). Hu, human samples; O-HFA, offspring of HFA mice; F, fecal sample; C, cecal sample; L, colon sample; y, years; w, weeks.

revealed that HDL could exist in HFA mice. Hirayama et al. (13) considered that the bacterial balance in the intestines of HFA mice might be controlled by physiological conditions of the mouse intestine and not by the balance of microbes in human feces. HDL in this study were most similar to *L. delbrueckii*. This bacterium can be established in the murine cecum (21, 38). Therefore, HDL may also be established in the intestines of humans and mice under different physiological

TABLE 3. Detection of HDL by use of each primer set

Sample no.	Time point[a](wk)	Tract[b]	Detection by primer set[c]:	
			Lac 1-Lac 2	HDL-f–Lac 2
HFA-1	1	F	+	ND
	2	F	+	ND
	4	F	+	+
	8	S	+	+
		C	+	ND
		L	+	ND
HFA-2	1	F	+	ND
	2	F	+	ND
	4	F	+	+
	8	S	+	+
		C	+	ND
		L	+	ND
HFA-3	1	F	+	ND
	2	F	+	+
	4	F	+	ND
	8	S	+	ND
		C	+	ND
		L	+	ND
HFA-4	1	F	+	ND
	2	F	+	ND
	4	F	+	ND
	8	S	+	ND
		C	+	+
		L	+	ND
HFA-5	1	F	+	ND
	2	F	+	ND
	4	F	+	+
	8	S	+	ND
		C	+	ND
		L	+	ND

[a] The time point after administration of human feces.
[b] Intestinal tracts of samples derived from HFA mice. F, feces; S, small intestine; C, cecum; L, large intestine.
[c] +, detected; ND, not detected by PCR.

conditions. Imaoka et al. (15) improved HFA mice for the evaluation of functional food, and they reported that the HFA mice with segmented filamentous bacteria were able to retain HDL for 14 days. In this study, the HDL were detected at random and regardless of time point or intestinal tract. Our results indicated that the intestines of HFA mice have difficulty in retaining HDL or that HDL are difficult to detect in intestinal samples from HFA mice.

This study showed the dynamics of human intestinal microbiota in formerly germfree mice, and the movement and persistence of many unidentified bacteria were also shown. These results indicated that although HFA mice reflect the composition of individual human intestinal bacteria, there are differences between dominant bacterial populations. Moreover, we revealed that HDL could be established in the HFA mouse intestine. This report showed the intestinal bacteria of HFA mice by the use of molecular techniques in regions and time points, and a new concept could therefore be introduced. The composition of intestinal microbiota of colonized HFA mice was selected from a limited sample of bacteria derived from human inoculum. This finding would be reflected by a host-bacterium interaction, physiological conditions, and diet differences between humans and mice. We need to further the establishment of a suitable model for study and to clarify the details of the interaction between the host and the bacteria based on this research.

ACKNOWLEDGMENT

This work was supported by a grant from the Junior Research Associate Program of RIKEN, Japan.

REFERENCES

1. **Altschul, S. F., W. Gish, W. Miller, E. W. Myers, and D. J. Lipman.** 1990. Basic local alignment search tool. J. Mol. Biol. **215**:403–410.
2. **Apajalahti, J. H. A., H. Kettunen, A. Kettunen, W. E. Holben, P. H. Nurminen, N. Rautonen, and M. Mutanen.** 2002. Culture-independent microbial community analysis reveals that inulin in the diet primarily affects previously unknown bacteria in the mouse cecum. Appl. Environ. Microbiol. **68**:4986–4995.
3. **Clement, B. G., and C. L. Kitts.** 2000. Isolating PCR-quality DNA from human feces with a soil DNA kit. BioTechniques **28**:640–646.
4. **Cole, J. R., B. Chai, T. L. Marsh, et al.** 2003. The Ribosomal Database Project (RDP-II): previewing a new autoaligner that allows regular updates and the new prokaryotic taxonomy. Nucleic Acids Res. **31**:442–443.
5. **Edwards, C. A., C. Rumney, M. Davies, A. M. Parrett, J. Dore, F. Martin, J. Schmitt, B. Stahl, E. Norin, T. Midtvedt, I. R. Rowland, P. Heavey, H. Köhler, B. Stocks, and H. Schroten.** 2003. A human flora-associated rat model of the breast-fed infant gut. J. Pediatr. Gastroenterol. Nutr. **37**:168–177.
6. **Fujiwara, S., T. Hirota, H. Nakazato, T. Mizutani, and T. Mitsuoka.** 1991. Effect of konjac mannan on intestinal microbial metabolism in mice bearing human flora and in conventional F344 rats. Food Chem. Toxicol. **29**:601–606.
7. **Gérard, P., F. Béguet, P. Lepercq, L. Rigottier-Gois, V. Rochet, C. Andrieux, and C. Juste.** 2004. Gnotobiotic rats harboring human intestinal microbiota as a model for studying cholesterol-to-coprostanol conversion. FEMS Microbiol. Ecol. **47**:337–343.
8. **Godon, J. J., E. Zumstein, P. Dabert, F. Habouzit, and R. Moletta.** 1997. Molecular microbial diversity of an anaerobic digestor as determined by small-subunit rDNA sequence analysis. Appl. Environ. Microbiol. **63**:2802–2813.
9. **Harris, M. A., C. A. Reddy, and G. R. Carter.** 1976. Anaerobic bacteria from the large intestine of mice. Appl. Environ. Microbiol. **31**:907–912.
10. **Hayashi, H., M. Sakamoto, M. Kitahara, and Y. Benno.** 2003. Molecular analysis of fecal microbiota in elderly individuals using 16A rDNA library and T-RFLP. Microbiol. Immunol. **47**:557–570.
11. **Heilig, H. G. H. J., E. G. Zoetendal, E. E. Vaughan, P. Marteau, A. D. L. Akkermans, and W. M. de Vos.** 2002. Molecular diversity of *Lactobacillus* spp. and other lactic acid bacteria in the human intestine as determined by specific amplification of 16S ribosomal DNA. Appl. Environ. Microbiol. **68**:114–123.
12. **Hirayama, K.** 1999. Ex-germfree mice harboring intestine microbiota derived from other animal species as an experimental model for ecology and metabolism of intestinal bacteria. Exp. Anim. **48**:219–227.
13. **Hirayama, K., K. Itoh, E. Takahashi, and T. Mitsuoka.** 1995. Comparison of composition of faecal microbiota and metabolism of faecal bacteria among 'human-flora-associated' mice inoculated with faeces from six different human donors. Microb. Ecol. Health Dis. **8**:199–211.
14. **Hirayama, K., K. Miyaji, S. Kawamura, K. Itoh, E. Takahashi, and T. Mitsuoka.** 1995. Development of intestinal flora of human-flora-associated (HFA) mice in the intestine of their offspring. Exp. Anim. **44**:219–222.
15. **Imaoka, A., H. Satoyama, A. Takagi, S. Matsumoto, and Y. Umesaki.** 2004. Improvement of human faecal flora-associated mouse model for evaluation of the functional foods. J. Appl. Microbiol. **96**:656–663.
16. **Itoh, K., T. Mitsuoka, K. Sudo, and K. Suzuki.** 1983. Comparison of fecal flora of mice based upon different strains and different housing conditions. Z. Versuchstierkd. **25**:135–146.
17. **Kibe, R., M. Sakamoto, H. Hayashi, H. Yokota, and Y. Benno.** 2004. Maturation of the murine cecal microbiota as revealed by terminal restriction fragment length polymorphism and 16S rRNA gene clone libraries. FEMS Microbiol. Lett. **235**:139–146.
18. **Lane, D. J.** 1991. 16S/23S rRNA sequencing, p. 115–175. *In* E. R. Stackebrandt and M. Goodfellow (ed.), Nucleic acid techniques in bacterial systematics. John Wiley and Sons Ltd., Chichester, United Kingdom.
19. **Lin, J. H., and D. C. Savage.** 1984. Host specificity of the colonization of murine gastric epithelium by lactobacilli. FEMS Microbiol. Lett. **24**:67–71.
20. **Liu, W. T., T. L. Marsh, H. Cheng, and L. J. Forney.** 1997. Characterization of microbial diversity by determining terminal restriction fragment length polymorphisms of genes encoding 16S rRNA. Appl. Environ. Microbiol. **63**:4516–4522.
21. **McConnell, M. A., and G. W. Tannock.** 1991. Lactobacilli and azoreductase activity in the murine cecum. Appl. Environ. Microbiol. **57**:3664–3665.

22. **Mengoni, A., E. Grassi, and M. Bazzicalupo.** 2002. Cloning method for taxonomic interpretation of T-RFLP. BioTechniques **33**:990–992.
23. **Mitsuoka, T.** 1982. Recent trends in research on intestinal flora. Bifidobacteria Microflora **1**:3–24.
24. **Morishita, Y., T. Mitsuoka, C. Kaneuchi, S. Yamamoto, and M. Ogata.** 1971. Specific establishment of Lactobacilli in the digestive tract of germ-free chickens. Jpn. J. Microbiol. **15**:531–538.
25. **Osborn, A. M., E. R. B. Moore, and K. N. Timmis.** 2000. An evaluation of terminal-restriction fragment length polymorphism (T-RFLP) analysis for the study of microbial community structure and dynamics. Environ. Microbiol. **2**:39–50.
26. **Paster, B. J., S. K. Boches, J. L. Galvin, R. E. Ericson, C. N. Lau, V. A. Levanos, A. Sahasrabudhe, and F. E. Dewhirst.** 2001. Bacterial diversity in human subgingival plaque. J. Bacteriol. **183**:3770–3783.
27. **Pearson, W. R., and D. J. Lipman.** 1988. Improved tools for biological sequence comparison. Proc. Natl. Acad. Sci. USA **85**:2444–2448.
28. **Raibaud, P., R. Ducluzeau, F. Dubos, S. Hudault, H. Bewa, and M. C. Muller.** 1980. Implantation of bacteria from the digestive tract of man and various animals into gnotobiotic mice. Am. J. Clin. Nutr. **33**:2440–2447.
29. **Roach, S., and G. W. Tannock.** 1980. Anaerobic fusiform shaped bacteria isolated from the caecum of conventional mice. J. Appl. Bacteriol. **48**:115–123.
30. **Rowland, I. R., and R. Tanaka.** 1993. The effects of transgalactosylated oligosaccharides on gut flora metabolism in rats associated with a human faecal microflora. J. Appl. Bacteriol. **74**:667–674.
31. **Rumney, C. J., and I. R. Rowland.** 1992. In vivo and in vitro models of the human colonic flora. Crit. Rev. Food Sci. Nutr. **31**:299–331.
32. **Sait, L., M. Galic, R. A. Strugnell, and P. H. Janssen.** 2003. Secretory antibodies do not affect the composition of bacterial microbiota in the terminal ileum of 10-week-old mice. Appl. Environ. Microbiol. **69**:2100–2109.
33. **Sakamoto, M., H. Hayashi, and Y. Benno.** 2003. Terminal restriction fragment length polymorphism analysis for human fecal microbiota and its application for analysis of complex bifidobacterial communities. Microbiol. Immunol. **47**:133–142.
34. **Sakamoto, M., Y. Takeuchi, M. Umeda, I. Ishikawa, and Y. Benno.** 2003. Application of terminal RFLP analysis to characterize oral bacterial flora in saliva of healthy subjects and patients with periodontitis. J. Med. Microbiol. **52**:79–89.
35. **Salzman, N. H., H. de Jong, Y. Paterson, H. J. Harmsen, G. W. Welling, and N. A. Bos.** 2002. Analysis of 16S libraries of mouse gastrointestinal microflora reveals a large new group of mouse intestinal bacteria. Microbiology **148**: 3651–3660.
36. **Stackebrandt, E., and B. M. Goebel.** 1994. Taxonomic note: a place for DNA-DNA reassociation and 16S rRNA sequence analysis in the present species definition in bacteriology. Int. J. Syst. Bacteriol. **44**:846–849.
37. **Suau, A., R. Bonnet, M. Sutren, J.-J. Godon, G. R. Gibson, M. D. Collins, and J. Dore.** 1999. Direct analysis of genes encoding 16S rRNA from complex communities reveals many novel molecular species within the human gut. Appl. Environ. Microbiol. **65**:4799–4807.
38. **Tannock, G. W., M. P. Dashkevicz, and S. D. Feighner.** 1989. Lactobacilli and bile salt hydrolase in the murine intestinal tract. Appl. Environ. Microbiol. **55**:1848–1851.
39. **Tannock, G. W., O. Szylit, Y. Duval, and P. Raibaud.** 1982. Colonization of tissue surfaces in the gastrointestinal tract of gnotobiotic animals by lactobacillus strains. Can. J. Microbiol. **28**:1196–1198.
40. **Walter, J., C. Hertel, G. W. Tannock, C. M. Lis, K. Munro, and W. P. Hammes.** 2001. Detection of *Lactobacillus*, *Pediococcus*, *Leuconostoc*, and *Weissella* species in human feces by using group-specific PCR primers and denaturing gradient gel electrophoresis. Appl. Environ. Microbiol. **67**:2578–2585.
41. **Wong, W. C., D. J. Hentges, and S. H. Dougherty.** 1996. Adequacy of the human faecal microbiota associated mouse as a model for studying the ecology of the human intestinal tract. Microb. Ecol. Health Dis. **9**:187–198.

Biosci. Biotechnol. Biochem., **69** (3), 638–641, 2005

Note

Molecular Monitoring of the Developmental Bacterial Community in the Gastrointestinal Tract of Japanese Infants

Prapa SONGJINDA,[1] Jiro NAKAYAMA,[1,†] Yumiko KUROKI,[1] Shigemitsu TANAKA,[1] Sanae FUKUDA,[2] Chikako KIYOHARA,[3] Tetsuro YAMAMOTO,[2,4] Kunio IZUCHI,[5] Taro SHIRAKAWA,[2] and Kenji SONOMOTO[1]

[1]*Laboratory of Microbial Technology, Division of Microbial Science and Technology, Department of Bioscience and Biotechnology, Faculty of Agriculture, Graduate School, Kyushu University, 6-10-1 Hakozaki, Higashi-ku, Fukuoka 812-8581, Japan*
[2]*Department of Health Promotion and Human Behavior, Kyoto University Graduate School of Public Health, Yoshida-Konoe cho, Sakyo-ku, Kyoto 606-8501, Japan*
[3]*Department of Preventive Medicine, Division of Social Medicine, Graduate School of Medical Sciences, Kyushu University, Maidashi 3-1-1, Higashi-ku, Fukuoka 812-8582, Japan*
[4]*Total Technology Consultant, 1-20-2 Ebisunishi, Shibuya-ku, Tokyo 150-0021, Japan*
[5]*Izuchi Hospital, 4-15-6 Yakuin, Chuo-ku, Fukuoka 810-0022, Japan*

Received October 18, 2004; Accepted November 26, 2004

The dynamics of the developmental bacterial community in the Japanese neonatal gastrointestinal tract were examined by monitoring 16S ribosomal RNA gene (rDNA) diversity in fecal samples by PCR and denaturing gradient gel electrophoresis (DGGE). The results showed a certain pattern common in infants without antibiotic treatment, in which aerobes, *e.g.*, *Pseudomonas*, appeared first and were then immediately replaced by facultative anaerobe, *Enterococcus*, *Streptococcus*, and *Enterobacteriaceae* through the first month, and finally strictly anaerobic *Bifidobactrerium* appeared.

Key words: denaturing gradient gel electrophoresis (DGGE); gastrointestinal tract; infant; 16S rRNA; intestinal microbiota

Soon after birth, bacterial colonization starts in the previously germfree gastrointestinal tract and commensal host-microbial relationships begin.[1,2] The colonizing bacteria contribute to maintenance of the mucosal barrier, facilitate carbohydrate assimilation, and modulate the mucosal immune system. Thus, the initial development of intestinal microbiota is considered to have great influence on the health of the infant. In this study, the succession of the gastrointestinal bacterial community was examined for the first two months in nine Japanese infants by monitoring 16S ribosomal RNA gene (rDNA) diversity in fecal samples.

All infant subjects (infants nos. 1, 2, 5, 6, 10, 20, 24, 25, and 33) participated in this study were vaginally delivered. Infant no. 5 was fed formula milk and the other infants were fed both breast and formula milk during the sampling period. Infants no. 1 and no. 33 were subjected to antibiotic therapy, receiving cefalex (50 mg/kg, 4 times a day) the first four days, whereas infant no. 5 was treated on day 0 only. Fecal samples were collected on day 0/1, day 3, day 5, month 1, and month 2 (there was no month-2 sample from infant no. 5). All the parents of our subjects gave written informed consent and the Ethics Committee of the Faculty of Medicine of Kyoto University approved this study protocol.

DNA was isolated from each fecal sample using a bead beating method essentially as previously described,[3] except for 2–3 times washing of the fecal sample before the bead beating step. In order to construct 16S rDNA libraries, a V1–V3 region of 16S rDNA was amplified from each sample by PCR with 8UA (5′-AGAGTTTGATCCTGGCTCAG-3′)[4] and 519B (5′-ATTACCGCSGCTGCTG-3′)[5] primers, and cloned into a pGEM-T vector (Promega, Madison, WI), and transformed in *E. coli* JM109. About ten clones from each library were sequenced. In total, 357 clones were sequenced and the ribotypes found are summarized with the result of the database search in Table 1.

PCR-denaturing gradient gel electrophoresis (PCR-DGGE), which allowed rapid and efficient molecular fingerprinting of gut microbiota,[3,6] was performed in order to monitor the succession of the infant fecal bacterial community. The variable region V2–V3 of 16S rDNA was amplified by PCR using primers HDA1-GC (5′-CGC CCG GGG CGC GCC CCG GGC GGG GCG

† To whom correspondence should be addressed. Tel/Fax: +81-92-642-3020; E-mail: nakayama@agr.kyushu-u.ac.jp

Table 1. List of Ribotypes Obtained in This Study

Ribotype	Closest sequence relative[a] (species)	% identity	Numbers			Accession no.
			clones	subjects	DGGE[b]	
Gram-positive facultative anaerobes						
Ef	*Enterococcus faecalis*	99.4	25	4	7	AY635946
Ss	*Streptococcus salivarius*	99.8	14	6	3	AY635947
Sp	*Streptococcus parasanguis*	96.4	12	3	7	AY635948
Se	*Staphylococcus epidermidis*	100.0	11	4	8	AY635949
Pa	*Propionibacterium avidum*	99.0	4	3	0	AY635950
Em	*Enterococcus faecium*	99.8	4	2	6	AY635951
Sa	*Streptococcus anginosus*	99.8	4	1	1	AY635952
Lg	*Lactobacillus gasseri*	99.8	2	2	0	AY635953
St	*Streptococcus thermophilus*	99.8	2	1	5	AY635954
Sm'	*Streptococcus mitis*	96.6	2	1	0	AY635955
Sm	*Streptococcus mitis*	99.0	1	1	4	AY635956
Sc	*Streptococcus cremoris*	99.1	1	1	3	AY635957
Si	*Streptococcus infantarius*	99.6	1	1	1	AY635958
Gram-positive strict anaerobes						
Cb	*Clostridium butyricum*	100.0	25	4	4	AY635959
Bd	*Bifidobacterium dentium*	99.0	11	5	5	AY635960
Bp	*Bifidobacterium pseudocatanulatum*	100.0	11	2	5	AY635961
Fm	*Finegoldia magna*	98.8	2	2	0	AY635962
Rm	*Ruminococcus* sp.	99.0	2	1	1	AY635963
Ch	*Clostridium hathewayi*	98.6	3	1	1	AY635964
Gram-positive aerobes						
Mm	*Micrococcus mucilaginosus*	98.8	5	2	1	AY635965
Ar	*Acinetobacter rhizospaerae*	98.7	5	1	0	AY635966
Gram-negative facultative anaerobes						
Es	*Enterobacter* sp. B901-2	99.8	32	5	6	AY635967
Kp	*Klebsiella pneumoniae*	99.2	31	6	2	AY635968
Km	*Klebsiella milletis*	99.0	19	8	6	AY635969
Ec	*Escherichia coli*	99.2	15	2	3	AY635970
Ko	*Klebsiella oxytoca*	99.6	12	2	2	AY635971
Cd	*Citrobacter diversus*	98.5	5	2	0	AY635972
Kr	*Klebsiella rennanqify*	99.0	9	3	4	AY635973
Cg	*Calymmatobacterium granulomatis*	99.0	7	4	1	AY635974
Ea	*Enterobacter aerogenes*	97.8	5	2	0	AY635975
Km'	*Klebsiella milletis*	99.0	3	3	1	AY635976
Sf	*Escherichia coli*	99.4	3	2	0	AY635977
Ko'	*Klebsiella oxytoca*	98.3	2	1	1	AY635978
Kr'	*Klebsiella rennanqify*	98.9	2	1	0	AY635979
Gram-negative strict anaerobes						
Bu	*Bacteroides uniformis*	99.4	8	3	1	AY635980
Vp	*Veillonella parvula*	98.9	1	1	1	AY635981
Vp'	*Veillonella parvula*	98.4	1	1	1	AY635982
Gram-negative aerobes						
Pm	*Pseudomonas marginalis/reactans/veronii*	99.4	28	5	5	AY635983
Fh	*Flavobacterium heparinum*	98.1	8	3	3	AY635984
Pt	*Pseudomonas tolaasii*	99.6	7	4	2	AY635985
Ad	*Acidovorax deflvii*	99.4	6	1	1	AY635986
Ph	*Phyllobacterium myrsinacearum*	99.6	4	1	0	AY635987
Pr	*Pseudomonas trivialis/poae*	99.6	2	2	2	AY635988

Ribotypes found with more than two clones in the 16S rDNA libraries or found only once but also detected in DGGE are listed.
[a]Cultured bacteria in Genbank showing highest identity as a result of Blast search.
[b]The number of bands corresponding to the indicated species in the DGGE (Fig. 1).

GGG GCA CGG GGG GAC TCC TAC GGG AGG CAG CAG T-3′) and HDA2 (5′-GTA TTA CCG CGG CTG CTG GCA C-3′).[7] The PCR condition was as follows: 94 °C for 5 min, 30 cycles consisting of 94 °C for 40 s, 58 °C for 20 s, and 72 °C for 1 min, and finally 72 °C for 5 min. DGGE analysis was performed as described by Muyzer *et al.*[8] and Heilig *et al.*[9] using a Dcode System apparatus (Bio-Rad, CA). Each band in the DGGE gel was assigned one of the ribotypes in Table 1 either by sequencing of DNA fragments excised from the DGGE gel or by comparing band positions with those of reference clones derived from the 16S rDNA clone library.

Figure 1 shows the DGGE profile of nine subjects. Although each subject showed individual banding patterns, a stepwise development from aerobic to

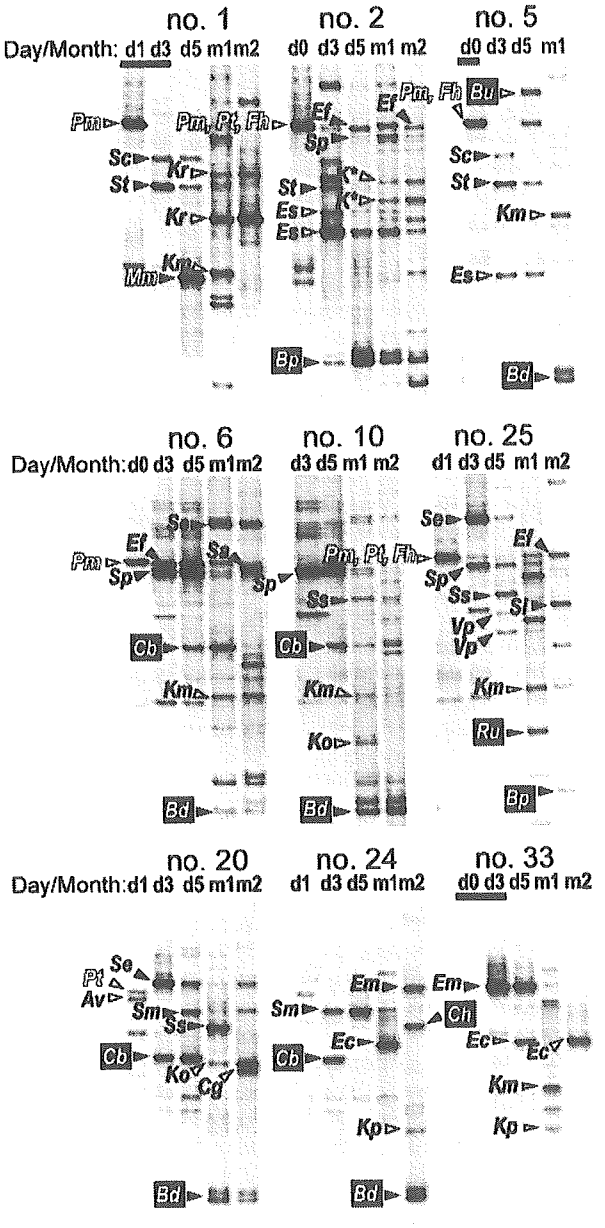

Fig. 1. PCR-DGGE Profiles Representing the Fecal Bacterial Community in the First Two Months of Nine Infants.

The bands identified with ribotypes in the 16S rDNA clone libraries are indicated by arrowheads with their names listed in Table 1, except K* which indicates unidentified *Klebsiella* spp. Open and black arrowheads represent Gram-negative and Gram-positive bacteria respectively. Open, black, and outlined letters represent aerobic, facultatively anaerobic, and strictly anaerobic bacteria respectively. Bold lines under the sampling days indicate the period of antibiotic treatment. Electrophoresis was done in 8% polyacylamide gel with a denaturing gradient of 30–65%, where 100% corresponds to 7 M urea and 40% formamide. The gel was run at 100 V for 6.5 h at 60 °C and then stained in 1 × SYBR Gold (Molecular Probes, Eugene, OR).

anaerobic microbial ecosystem was observed in the succession of bacterial composition in the seven subjects (nos. 2, 5, 6, 10, 20, 24, and 25) without successive antibiotic treatment in the first four days. In the beginning, bands corresponding to aerobic Gram-negative bacteria such as *Pseudomonas* appeared and they were then replaced by facultatively anaerobic bacteria such as *Streptococcus*, *Enterococcus*, or *Staphylococcus epidermidis* and *Enterobacteriaceae*. Particularly, strong bands closely related to *Streptococcus parasanguis*, *Streptococcus cremoris* and *Streptococcus thermophilus* appeared on day 3 in many subjects. It is interesting to note that a large majority of the bacteria types such as *Streptococcus parasanguis*, *Streptococcus mitis*, *Streptococcus salivarius*, *Bifidobacterium dentium*, and *Veillonella parvula* detected in this period are regarded as oral-origin bacteria rather than intestinal species. This suggests that these oral-origin bacteria may transiently colonize the intestine during this period.

Bifidobacteria detected in the bottom part of the DGGE gel appeared within two months in most subjects. In infant no. 2, *Bifidobacterium pseudocatanulatum* colonized predominantly from day 3 and continued until 2 months of age. This subject was only the case which agreed with the finding of previous studies,[6,10,11] showing that bifidobacteria usually appear and become dominant within a week after birth. The appearance of bifidobacterial bands in infant no. 2 was concomitant with a decrease in *Enterobacteriaceae* bands, which appeared as dominant on day 3. A concomitant decrease in *Enterobacteriaceae* with an increase of bifidobacteria in breast-milk fed infants has been reported.[12] Bands related to *Clostridium butyricum* were also detected in infants nos. 6, 10, 20, and 24, in which they appeared earlier than bifidobacteria. The other strict anaerobes, *Veillonella parvula*-like bacteria, and *Ruminococcus* sp. were found only in infant no. 25. *Bacteroides uniformis* was detected only at day 5 in infant no. 5 (antibiotic treatment on day 0) who was the only subject brought up only on formula milk.

Infants nos. 1 and 33 treated with antibiotics in the first 3 days showed relatively simple microbiota, and the developmental patterns deviated remarkably from the trends observed in the other subjects without antibiotic treatment. In infant no. 1, a dominant band corresponding to *Micrococcus mucilaginosus*, which is not a common inhabitant of the intestine, appeared suddenly on day 5 and completely disappeared during month 1. In infant no. 33, a dominant band corresponding to *Enterococcus faecium* appeared on day 3 and disappeared during month 1. No bands corresponding to bifidobacteria and other strict anaerobes were found in the testing period in either baby and only bands corresponding to *Enterobacteriaceae* were found during month 1 and month 2, suggesting domination by *Enterobacteriaceae*. This was also indicated by the data of random sequencing of 16S rDNA clone libraries, which showed that all 30 clones sequenced from the month-1 and month-2 libraries of these two subjects belonged to *Enterobacteriaceae*. These data showed that antibiotic treatment at the beginning of life has strong

influence on the establishment of a normal microbial ecosystem in the intestine.

In conclusion, this molecular study indicates the stepwise development from aerobic to anaerobic microbial ecosystem with a variety of bacterial groups, although the process differed among individuals at the species level. The step of the bacterial colonization in the gastrointestinal tract is most likely a key to the developmental process. Strong antibiotic treatment interrupted the development of normal microbiota, including bifidobacteria. Further studies with modern molecular methods are needed for understanding of the environmental and host factors affecting the developmental process of neonatal microbiota.

Acknowledgment

We thank all the families who provided fecal samples for this study. This research was supported in part by a Research Grant for Immunology, Allergy, and Organ Transplants from the Ministry of Health and Welfare of Japan, by a grant from Danon Institute for the Promotion of Health and Nutrition, and by a grant from Takeda Science Foundation.

References

1) Mackie, R. I., Sghir, A., and Gaskins, H. R., Developmental microbial ecology of the neonatal gastrointestinal tract. *Am. J. Clin. Nutr.*, **69** (Suppl.), 1035S–1045S (1999).
2) Hooper, L. V., and Gordon, J. I., Commensal host-bacterial relationships in the gut. *Science*, **292**, 1115–1118 (2001).
3) Zoetendal, E. G., Akkermans, A. D. L., and de Vos, W. M., Temperature gradient gel electrophoresis analysis of 16S rRNA from human fecal samples reveals stable and host-specific communities of active bacteria. *Appl. Environ. Microbiol.*, **64**, 3854–3859 (1998).
4) Acinas, S. G., Anton, J., and Rodrigues-Valera, F., Diversity of free-living and attached bacteria in offshore western Mediterranean waters as depicted by analysis of genes encoding 16S rRNA. *Appl. Environ. Microbiol.*, **65**, 514–522 (1999).
5) Bertilsson, S., Cavanaugh, C. M., and Polz, M. F., Sequencing-independent method to generate oligonucleotide probes targeting a variable region in bacterial 16S rRNA by PCR with detachable primers. *Appl. Environ. Microbiol.*, **68**, 6077–6086 (2002).
6) Favier, C. F., Vaughan, E. E., de Vos, W. M., and Akkermans, A. D. L., Molecular monitoring of succession of bacterial communities in human neonates. *Appl. Environ. Microbiol.*, **68**, 219–226 (2002).
7) Tannock, G. W., Munro, K., Harmsen, H. J. M., Welling, G. W., Smart, J., and Gopal, P. K., Analysis of the fecal microflora of human subjects consuming a probiotic product containing *Lactobacillus rhamnosus* DR20. *Appl. Environ. Microbiol.*, **66**, 2578–2588 (2000).
8) Muyzer, G., de Vaal, E., and Uitterlinden, A., Profiling of complex microbial populations by denaturing gel electrophoresis analysis of polymerase chain reaction-amplified genes coding for 16S rRNA. *Appl. Environ. Microbiol.*, **59**, 695–700 (1993).
9) Heilig, H. G. H. J., Zoetendal, E. G., Vaughan, E. E., Marteau, P., Akkermans, A. D. L., and de Vos, W. M., Molecular diversity of *Lactobacillus* spp. and other lactic acid bacteria in the human intestine as determined by specific amplification of 16S ribosomal DNA. *Appl. Environ. Microbiol.*, **68**, 114–123 (2002).
10) Benno, Y., and Mitsuoka, T., Development of intestinal microflora in humans and animals. *Bifidobacteria Microflora*, **5**, 13–25 (1986).
11) Weiling, G. W., Wildeboer-Veloo, L., Raangs, G. C., Franks, A. H., Jansen, G. J., Tonk, R. H. J., Degener, J. E., and Harmsen, H. J. M., Variations of bacterial populations in human feces measured by FISH with group-sepcific 16S rRNA-targeted oligonucleotide probes. In "Molecular Ecological Detection and Identification of Intestinal Microflora", ed. Mitsuoka, T., Japan Scientific Societies Press, Tokyo, pp. 7–18 (2000).
12) Yoshioka, H., Iseki, K., and Fugita, K., Development and differences of intestinal flora in the neonatal period in breast-fed and bottle-fed infants. *Pediatrics*, **72**, 317–321 (1983).

Clinical and Experimental Immunology ORIGINAL ARTICLE doi:10.1111/j.1365-2249.2005.02805.x

Distinct gene expression patterns of peripheral blood cells in hyper-IgE syndrome

T. Tanaka,* H. Takada,* A. Nomura,* S. Ohga,* R. Shibata† and T. Hara*
*Department of Paediatrics, Graduate School of Medical Sciences, Kyushu University and †Department of Paediatrics, Fukuoka National Hospital, Fukuoka, Japan

Accepted for publication 24 February 2005
Correspondence: Hidetoshi Takada, Department of Paediatrics, Graduate School of Medical Sciences, Kyushu University, 3-1-1, Maidashi, Higashi-ku, Fukuoka, 812–8582, Japan.
E-mail: takadah@pediatr.med.kyushu-u.ac.jp

Summary

Hyper-immunoglobulin E (IgE) syndrome (HIES) is one of the primary immunodeficiency syndromes. Although the cytokine dysregulation is suggested to play a role in its pathophysiology, the causative gene has not yet been identified. To investigate the pathophysiology and candidate genes involved in this disease, we performed microarray analysis of unstimulated peripheral $CD4^+$ T cells and $CD14^+$ cells, as well as peripheral blood mononuclear cells (PBMNC) stimulated with *Staphylococcus aureus* isolated from HIES patients and healthy controls. By microarray analysis, 38 genes showed over 2-fold differences between the HIES patients and healthy controls in purified $CD14^+$ cells, although only small differences in the gene expression profiles were observed between the two groups in purified $CD4^+$ T cells. *RGC32* expression levels showed the greatest difference between the two groups, and were significantly elevated in HIES compared with those in severe atopic dermatitis or healthy controls using real-time PCR. A significantly larger number of lysosome-related genes were up-regulated, and significantly larger number of genes related to cell growth and maintenance were down-regulated in HIES. After the stimulation of PBMNC with *Staphylococcus aureus*, 51 genes showed over 3-fold differences between HIES patients and healthy controls. A significantly large number of immunoglobulin-related genes were up-regulated in HIES. The distinct patterns of gene expression profiles and *RGC32* expression levels will be useful for understanding the pathophysiology and for diagnosis of HIES, respectively.

Keywords: hyper-immunoglobulin E syndrome, microarray/ genomics/ proteomics, immunodeficiency–primary

Introduction

Hyper-immunoglobulin E (IgE) syndrome (HIES) is a rare primary immunodeficiency, characterized by severe recurrent staphylococcal infections, eczema, and markedly elevated levels of IgE [1,2]. Pneumatoceles, dental and skeletal abnormalities and neutrophil defects are sometimes observed in patients with HIES [3,4]. Since the causative gene of HIES has not been identified, the diagnosis of HIES is sometimes difficult because of the similarity of symptoms to severe atopic dermatitis, particularly during early infancy.

Previous studies suggested that there might be a Th1/Th2 imbalance, especially a defect in Th1 induction [5–9], which may account for the high serum levels of IgE and eosinophilia in HIES. In other reports, mitogen-induced secretion of IL-4 and IFN-γ by PBMNC was not different between patients with HIES and healthy controls [10,11]. Susceptibilities to bacterial and fungal infections in HIES indicate possible defects in phagocytes and T cells, while bone and dental abnormalities suggest certain defects in monocyte-lineage cells such as osteoclasts and osteoblasts.

Thus, to assess the pathogenesis and pathophysiology of the HIES, we purified $CD4^+$ T cells and $CD14^+$ cells from HIES patients and analysed the whole gene expression with microarray. HIES showed characteristic gene expression patterns compared with controls. Analysis of distinct gene expression patterns would be useful in the understanding of the pathophysiology as well as in the diagnosis of HIES.

Methods

Patients

Eight patients (median age 16·5 years, range 5–34 years; 3 males and 5 females) with HIES were enrolled in this study. The patients' characteristics are shown in Table 1. The samples obtained from patients 4 and 7 (Table 1) were used in the microarray analysis. As the controls, peripheral blood was obtained from 17 age-matched patients with severe atopic dermatitis (median age 8 years, range 1·0–34 years; 11 males and 6 females) and 15 healthy donors (median age 11 years, range 3–20 years, 8 males and 7 females). All the atopic patients had typical skin manifestation with increased serum levels of IgE (range 183–19504 IU/ml, median 3438 IU/ml) with or without eosinophilia (range 308–2018/μl, median 860/μl), and did not have the recurrent infection, lung cyst, abnormal facies, or bone abnormalities. The median values (ranges) of points of HIES diagnosis scoring system [12] were 25 (18–31) in HIES patients, and 16 (4–25) in atopic dermatitis patients ($P < 0{\cdot}01$, by Mann–Whitney's test). Informed consent was obtained from all patients and healthy donors. This study was approved by Regional Committee of Ethics for Human research at Faculty of Medicine of Kyushu University.

Isolation of $CD4^+$ T cells and $CD14^+$ cells

PBMNC were separated immediately using density-gradient centrifugation using LSM (Cappel-ICN Immunobiologicals, Costa Mesa, CA, USA). $CD4^+$ T cells were purified using cell sorter (EPICS ALTRA; Beckman Coulter, Hialeah, FL, USA) after staining with phycoerythrin (PE)-conjugated anti-CD4 antibody (Beckman Coulter). $CD14^+$ cells were isolated using CD14 MicroBeads (Miltenyi Biotec GmbH, Bergisch Gladbach, Germany). The purity of $CD4^+$ T cells or $CD14^+$ cells was higher than 97%.

PBMNC stimulation with *Staphylococcus aureus*

PBMNC were incubated in 48 well-culture plates at the concentration of 1×10^6 cells/ml. Heat killed *Staphylococcus aureus* (frozen at the concentration of 1×10^9 CFU/ml) was added at the concentration of 1×10^7 CFU/ml. After 6 h, the cells were harvested, washed twice with phosphate buffered saline, and used for total RNA extraction.

RNA extraction, amplification and labelling

Total RNA was extracted using Isogen (Nippon Gene, Tokyo, Japan). For the microarray analysis of purified $CD4^+$ T cells or $CD14^+$ cells, linear amplification of RNA was carried out using an Amino Allyl Message Amp aRNA Kit (Ambion, Austin, TX, USA). Briefly, double-stranded complementary DNA (cDNA) was synthesized from total RNA using oligo

Table 1. Clinical characteristics of the patients with HIES.

Patient	Age	Gender	Eczematous rash	Skin abscesses	Lymphadenitis	Pneumonia	Lung cyst	Characteristic facies	Retained primary teeth	Fractures with minor trauma	Articular over-extension	Scoliosis	Serum IgE level (IU/ml)	*St. aureus* -specific IgE (U/ml)*	Eosinophil count (cells/μl)
1	5y	Female	+	+	+	+	–	+	–	–	+	–	40100	2260	2088
2	9y	Male	+	+	+	+	–	+	–	+	–	+	27180	1675	9520
3	11y	Male	+	+	+	+	–	–	–	–	–	–	17420	1331	1884
4	16y	Female	+	+	+	+	+	+	+	+	–	–	37780	2219	1198
5	17y	Female	+	+	–	+	–	+	–	–	–	+	16000	460	3663
6	18y	Female	+	+	+	+	–	+	–	–	–	–	24807	2305	1064
7	18y	Female	+	+	+	+	+	+	+	–	–	+	18300	716	18300
8	34y	Male	+	+	+	+	–	–	+	+	+	–	28100	14530	1480

*Normal range: < 400 U/ml.

dT primer with a T7 RNA polymerase promoter site added to the 3′ end. Then, *in vitro* transcription was performed in the presence of amino allyl UTP to produce multiple copies of amino allyl labelled complementary RNA (cRNA). Amino allyl labelled cRNA was purified, and then 15 μg of cRNA was reacted with N-hydroxy succinimide esters of Cy3 (Amersham Pharmacia Biotech, Piscataway, NJ, USA) for cRNA from the purified cells, and Cy5 (Amersham Pharmacia Biotech) for that from 5 control PBMNC, according to the protocol of Hitachi Software Engineering (Yokohama, Japan).

For the gene expression analysis of PBMNC before and after the stimulation with *Staphylococcus aureus*, cDNA microarray was applied. After the linear amplification using RiboAmp RNA Amplification Kit (Arcturus Bioscience Mountain View, CA, USA), FluoroLink Cy3-dUTP- or FluoroLink Cy5-dUTP-labelled cDNA was synthesized using RNA Fluorescence Labeling Core Kit (M-MLV version) ver.2·0 (Takara Bio, Tokyo Japan), according to the manufacturer's instructions.

Microarray analysis

Microarray analysis for the purified $CD4^+$ T cells and $CD14^+$ cells was performed using an AceGene Human Oligo Chip 30K (Hitachi Software Engineering) that contains approximately 30 000 genes. Each gene expression level of $CD4^+$ T cells and $CD14^+$ cells from the patients or controls was determined by comparison with that from the standard sample. The arrays were scanned by FLA-8000 (Fuji Photo Film, Tokyo, Japan), and changed to the numerical values by ArrayVision (Amersham Biosciences). The numerical data were normalized using LOWESS method. In the microarray analysis of $CD4^+$ T cells, data from 2 HIES patients and those from 2 healthy controls were compared. In the analysis of $CD14^+$ cells, data from 2 HIES patients were compared with those from 2 healthy controls and one with severe atopic dermatitis to find out genes that were expressed specifically in HIES. Genes that were consistently up-regulated or consistently down-regulated in both HIES patients compared with all controls, and that showed over 2·0-fold differences by the comparison between the two groups in the mean expression levels were selected.

For the microarray analysis of PBMNC before and after the stimulation with *Staphylococcus aureus*, Agilent Human 1 cDNA Microarray (Agilent Technology, Palo Alto, CA, USA) was used, which contains 13 767 genes. The changes of the gene expression were analysed by direct comparison of the samples before and after the stimulation with *Staphylococcus aureus* in two patients with HIES, 2 healthy controls. The data were scanned by FLA-8000 (Fuji Photo Film), and changed to the numerical values by ArrayVision (Amersham Biosciences). The ratios of each gene expression level before and after the stimulation were obtained and normalized by being divided by the median value in each plate. Genes that were expressed consistently higher or consistently lower in both HIES patients compared with all controls, and that showed over 3·0-fold differences by the comparison between the two groups in the mean expression levels were selected.

The data with low signal-to-noise ratios ($S/N < 3$) were not used for further analysis. The data were analysed using Gene Spring software (Silicon Genetics, Redwood City, CA, USA).

Real-time PCR

An Assay-on-Demand Gene Expression Product Hs.00204129_m1 (Applied Biosystems) was used for primers and probes for *response gene to complement 32* (*RGC32*). A Pre-Developed TaqMan Assay Reagent Human ACTB (β-actin) (Applied Biosystems) was used for the internal control. TaqMan assay was performed according to the manufacturer's instructions. In brief, PCR primer set and TaqMan probe for the target gene were added in the TaqMan Universal PCR Master Mix (Applied Biosystems) at the final volume of 25 μl. PCR condition was as follows: 50°C for 2 min and 95°C for 10 min, followed by 50 cycles of amplification at 94°C for 15 s and 60°C for 1 min. PCR amplification and the detection of the amounts of PCR products were performed by ABI PRISM 7700 Sequence Detector (Applied Biosystems). The gene expression levels were described by the relative ratios of the levels of target genes to those of the internal control (β-actin gene).

Statistical analyses

Chi-square test was used to analyse the deviated distribution of genes in each Gene Ontology into the two groups. One-way ANOVA test was used for the comparison of gene expression levels in three groups, and comparison of the two groups among 3 was performed with Scheffe's test. The differences were considered to be significant when the P-value $< 0·05$.

Results

To evaluate the gene expression profiles of circulating $CD4^+$ T cells and $CD14^+$ cells (monocytes) from patients with HIES, we extracted mRNAs from purified cells and performed microarray analysis, together with those from non-HIES controls. Six up-regulated and 4 down-regulated genes in HIES showed over 2-fold differences compared with controls in $CD4^+$ T cells (Table 2), while 33 up-regulated and 5 down-regulated genes in HIES showed over 2-fold differences compared with controls in $CD14^+$ cells (Table 3). The expression levels of major Th1- or Th2-related genes in $CD4^+$ T cells and $CD14^+$ cells did not show more than 2-fold differences between HIES patients and controls (Tables 2 and 3). In addition, there were only small differences in the expression levels of most cytokine-related genes between

Table 2. Microarray analysis of purified $CD4^+$ T cells between HIES and healthy controls.

Gene name	Synonyms	GeneBank	*Fold difference
HIES > Control			
Haemoglobin, delta	HBD	NM_000519	2·4 (3·0, 2·0)
Chromosome 6 open reading frame 111	C6orf111	AF161424	2·3 (2·5, 2·1)
Haemoglobin, alpha 2	HBA2	AF281258	2·3 (2·5, 2·1)
No name		XM_031045	2·2 (2·2, 2·2)
Dynein, cytoplasmic, light intermediate polypeptide 2	DNCLI2	NM_006141	2·2 (2·8, 1·7)
Topoisomerase-related function protein 4–2		AF089897	2·0 (2·2, 1·9)
HIES < Control			
Polymerase (RNA) II (DNA directed) polypeptide D	POLR2D	BC010427	1/3·7 (1/3·8, 1/3·6)
No name		AC026785·3.13728·33112·2	1/2·3 (1/2·7, 1/1·9)
Sarcoglycan, gamma (35 kDa dystrophin-associated glycoprotein)	SGCG	NM_000231	1/2·3 (1/2·7, 1/1·9)
No name		U82695·2.1·167460·8	1/2·0 (1/2·6, 1/1·6)

*The difference of mean gene expression levels between 2 HIES patients and 2 healthy controls in microarray analysis is given. Values in parentheses are the fold differences of the gene expression in each HIES patient compared with the mean expression value in healthy controls. Genes that showed more than 2 fold expressional differences between HIES and healthy controls were selected.

HIES patients and controls (data, not shown). Among genes with over 2-fold differences in the expression between HIES patients and controls, there was no gene with a functional relevance to the abnormalities of bone and neutrophils, and increased serum levels of IgE, which might directly relate to the pathogenesis of HIES.

The expression levels of most up-regulated or down-regulated genes in $CD14^+$ cells that showed over 2-fold differences between HIES patients and controls were confirmed by real-time quantitative PCR. The expression levels of *RGC32*, with the highest expression among 33 up-regulated genes in HIES in $CD14^+$ cells by microarray analysis (Table 3), were significantly increased in PBMNC of HIES patients, compared with those in patients with atopic dermatitis or controls (Fig. 1). We were not able to analyse the expression levels of *DNCL1* (dynein, cytoplasmic, light polypeptide 1) gene, with the lowest expression among 5 down-regulated genes in HIES in $CD14^+$ cells by microarray analysis (Table 3), because the primers and probe were unable to be set to obtain precise and reproducible results due to the presence of many cDNA-type pseudogenes.

We compared the genes expressed in $CD4^+$ T cells or $CD14^+$ cells between HIES patients and controls, according to Gene Ontology Classifications from Gene Ontology Consortium to assess the differences in functionally related gene groups. At first, the genes that showed consistent expressional differences between HIES patients and controls in the two individual experiments were selected (HIES > normal: 1507 genes, HIES < control: 1116 genes). Among them, statistical analysis was performed in each gene group by the χ^2 test (Table 4). In unstimulated $CD4^+$ T cells, there were no gene groups which showed significant expressional differences between HIES patients and controls (data not shown). In unstimulated $CD14^+$ cells, a significantly larger number of lysosome-related genes was up-regulated (26 (1·73%) of 1507 total up-regulated genes, $P < 0·05$), and a significantly larger number of genes related to the cell growth and maintenance was down-regulated (246 (22·0%) of 1116 total down-regulated genes, $P < 0·05$) in HIES (Table 4).

Recurrent staphylococcal infection is one of the characteristics of patients with HIES. We stimulated PBMNC with heat-killed *Staphylococcus aureus*, and analysed the alteration of mRNA expression levels in HIES patients and healthy controls. Table 5 shows the genes with over 3·0-fold differences in the expression between HIES patients and controls before and after *Staphylococcus aureus* stimulation. Among

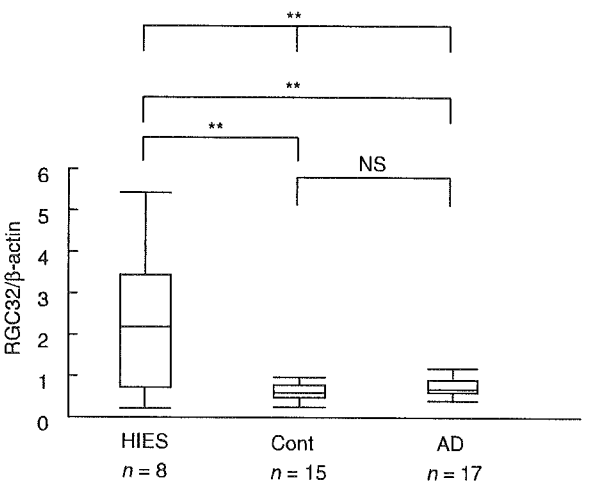

Fig. 1. Comparison of *RGC32* expression in patients with HIES, severe atopic dermatitis, and healthy controls. *RGC32* expression in PBMNC was analysed by real-time PCR. HIES: patients with HIES, Cont: healthy controls, AD: patients with severe atopic dermatitis, NS: not significant. Whiskers indicate the ranges, boxes the 25th to 75th percentiles and horizontal bars inside boxes the median values. Three groups were compared using One-way ANOVA test and each two groups were compared using Scheffe's test. $**P < 0·01$.

Table 3. Microarray analysis of purified CD14$^+$ cells between HIES and healthy controls.

Gene name	Synonyms	GeneBank	*Fold difference
HIES > Control			
Response gene to complement 32	RGC32	NM_014059	3·8 (4·2, 3·5)
Homeo box A1	HOXA1	NM_005522	3·8 (3·9, 3·7)
Cathepsin L	CTSL	NM_001912	3·2 (2·1, 4·8)
C-type lectin, superfamily member 2 (activation-induced)	CLECSF2	NM_005127	3·1 (1·8, 5·3)
Epstein-Barr virus induced gene 2	EBI2	NM_004951	2·9 (2·8, 2·9)
Fatty acid binding protein 5 (psoriasis-associated)	FABP5	NM_001444	2·8 (1·6, 5·0)
Myristoylated alanine-rich protein kinase C substrate	MARCKS	XM_047795	2·6 (2·2, 3·2)
Interleukin 1 receptor, type II	IL1R2	NM_004633	2·6 (3·4, 1·9)
Adaptor-related protein complex 3, sigma 1 subunit	AP3S	XM_003926	2·4 (2·6, 2·3)
CD3D antigen, delta polypeptide (TiT3 complex)	CD3D	M12727	2·4 (1·6, 3·7)
Carboxypeptidase, vitellogenic-like	CPVL	AF106704	2·4 (3·2, 1·8)
Receptor-interacting serine-threonine kinase 2	RIPK2	NM_003821	2·3 (3·0, 1·8)
Hypothetical protein FLJ20186	FLJ20186	NM_017702	2·3 (1·5, 3·7)
Protein tyrosine phosphatase, receptor type, E	PTPRE	NM_006504	2·3 (2·5, 2·1)
X Kell blood group precursor-related, Y-linked	XKRY	NM_004677	2·3 (3·1, 1·6)
Toll-like receptor 1	TLR1	NM_003263	2·3 (1·8, 2·8)
Spermidine/spermine N1-acetyltransferase	SAT	BC002503	2·2 (2·7, 1·9)
KIAA0431 protein	KIAA0431	NM_015251	2·2 (2·0, 2·4)
Vimentin	VIM	NM_003380	2·2 (2·8, 1·8)
Pleckstrin homology, Sec7 and coiled-coil domains, binding protein	PSCDBP	NM_004288	2·2 (2·3, 2·0)
Recombining binding protein suppressor of hairless (Drosophila)	RBPSUH	NM_015874	2·2 (1·6, 2·9)
Proteasome (prosome, macropain) 26S subunit, non-ATPase, 12	PSMD12	AB003103	2·2 (2·4, 1·9)
Multiple ankyrin repeats, single KH-domain (MASK) homolog	MASK	NM_024668	2·2 (2·5, 1·9)
Ubiquitin-conjugating enzyme E2B (RAD6 homolog)	UBE2B	NM_003337	2·2 (1·6, 2·8)
Syndecan 2	SDC2	AK025488	2·2 (1·6, 2·8)
Sialyltransferase 10 (alpha-2,3-sialyltransferase VI)	SIAT10	XM_044802	2·1 (1·8, 2·6)
Rearranged L-myc fusion sequence	RLF	NM_012421	2·1 (2·2, 2·0)
RAB6 interacting protein 1	RAB6IP1	AK025499	2·1 (2·5, 1·8)
No name		XM_008071	2·1 (2·0, 2·2)
CDC-like kinase 1	CLK1	NM_004071	2·1 (2·5, 1·7)
Hypothetical protein FLJ22965	FLJ22965	NM_022101	2·1 (2·2, 1·9)
Hypothetical protein CL25022	CL25022	AF131802	2·0 (1·8, 2·3)
Opioid growth factor receptor-like 1	OGFRL1	NM_024576	2·0 (2·2, 1·8)
HIES < Control			
Dynein, cytoplasmic, light polypeptide 1	DNCL1	NM_003746	1/2·9 (1/1·9, 1/4·4)
Calmodulin regulated spectrin-associated protein 1	CAMSAP1	NM_018627	1/2·4 (1/1·7. 1/3·2)
Placenta-specific 8	PLAC8	NM_016619	1/2·1 (1/1·6, 1/2·8)
Vacuolar protein sorting 35 (yeast)	VPS35	NM_018206	1/2·0 (1/1·6, 1/2·6)
Butyrophilin, subfamily 3, member A1	BTN3A1	NM_007048	1/2·0 (1/1·5, 1/2·8)

*The difference of mean gene expression levels between 2 HIES patients and 3 controls (2 healthy donors and a atopy patient) in microarray analysis is given. Values in parentheses are the fold differences of the gene expression in each HIES patient compared with the mean expression value in controls. Genes that showed more than 2 fold expressional differences between HIES and healthy controls were selected.

Table 4. Comparison of gene expression according to the Gene Ontology groups.

	HIES > Control	HIES < Control	*P*-value*
CD14$^+$ cells	(1507 genes)	(1116 genes)	
Lysosome related genes (total 137 genes)	26 (1·73%)	8 (0·72%)	< 0·05
Genes related to the cell growth and maintenance (total 2572 genes)	254 (16·9%)	246 (22·0%)	< 0·01
MNC stimulated with *Staphylococcus aureus*	(1194 genes)	(1331 genes)	
Immunoglobulin-related genes (total 54 genes)	29 (2·43%)	4 (0·30%)	< 0·01

*χ^2 test.

Table 5. Microarray analysis of the change of gene expression after the stimulation with *Staphylococcus aureus*.

Gene name	Synonyms	Gene bank	Fold increase of gene expression*		Fold difference**
			HIES	Control	HIES/Control
HIES > Control					
Ubinuclein 1	UBN1	AF108460	3·5	1/1·4	4·9 (5·0, 4·9)
Rho guanine nucleotide exchange factor (GEF) 1	ARHGEF1	Y09160	2·7	1/1·7	4·7 (2·7, 8·3)
Hydroxymethylbilane synthase	HMBS	X04808	3·4	1/1·3	4·3 (1·4, 13)
Bromodomain containing 3	BRD3	D26362	2·5	1/1·6	4·0 (3·7, 4·4)
Incyte EST			2·9	1/1·3	3·9 (2·8, 5·2)
KIAA0582 protein	KIAA0582	AK000856	1·3	1/3·0	3·8 (3·4, 4·2)
A kinase (PRKA) anchor protein (yotiao) 9	AKAP9	NM_005751	2·1	1/1·8	3·7 (4·6, 2·9)
Haloacid dehalogenase-like hydrolase domain	HDHD1A	M86934	2·6	1/1·4	3·7 (1·3, 11)
KIAA0555 gene product		AL137976	5·1	1·4	3·7 (2·3, 5·8)
Ral GEF with PH domain and SH3 binding motif 2	RALGPS2	AK001106	1·6	1/2·2	3·6 (3·2, 3·9)
Tripartite motif-containing 2	TRIM2	AB011089	1·5	1/2·4	3·5 (2·6, 4·7)
Serine (or cysteine) proteinase inhibitor, member 1	SERPINI1	NM_005025	2·1	1/1·6	3·5 (7·9, 1·5)
Cysteine conjugate-beta lyase; cytoplasmic	CCBL1	X82224	1·4	1/2·4	3·4 (3·3, 3·5)
Homeo box A7	HOXA7	AJ005814	3·2	1·0	3·3 (3·7, 3·0)
Scaffold attachment factor B2	SAFB2	D50928	3·3	1·0	3·3 (4·5, 2·4)
5′-nucleotidase, ecto (CD73)	NT5E	X55740	1·4	1/2·3	3·3 (3·7, 2·9)
Mad4 homolog		AL040187	1·4	1/2·3	3·3 (3·3, 3·3)
Aldo-keto reductase family 1, member C1	AKR1C1	M86609	5·8	1·8	3·3 (2·5, 4·3)
Hypothetical protein FLJ13213	FLJ13213	AK000867	2·6	1/1·3	3·3 (4·5, 2·4)
Human FLI1 gene for ERGB transcription fuctor		AB012624	2·0	1/1·6	3·3 (3·1, 3·4)
Myosin XVB, pseudogene	MYO15B	AK026339	1·3	1/2·5	3·2 (3·3, 3·2)
Adducin 2 (beta)	ADD2	S81079	1·6	1/2·0	3·2 (2·5, 4·2)
Zinc finger protein 236	ZNF236	AF085244	1·7	1/1·9	3·2 (4·1, 2·5)
Yippee-like 1 (Drosophila)	YPEL1	AW006162	3·1	1·0	3·2 (2·0, 5·1)
Incyte EST			1·1	1/3·0	3·2 (3·3, 3·0)
NIMA (never in mitosis gene a)-related kinase 1	NEK1	AL050385	3·3	1·1	3·1 (5·0, 2·0)
Protocadherin 9	PCDH9	AF169692	1·7	1/1·8	3·1 (4·2, 2·3)
Poly (ADP-ribose) polymerase family, member 2	ADPRTL2	AK001980	2·1	1/1·4	3·0 (3·2, 2·8)
Calcium/calmodulin-dependent protein kinase (CaM kinase) II delta	CAMK2D	AF071569	1·5	1/2·0	3·0 (1·7, 5·3)
HIES < Control					
Solute carrier organic anion transporter family, member 1A2	SLCO1A2	U21943	1·8	24	1/14 (1/29, 1/6·7)
Normal mucosa of oesophagus specific 1	NMES1	AK026298	4·6	37	1/8·1 (1/10, 1/6·3)
Syndecan 2	SDC2	J04621	4·1	23	1/5·6 (1/12, 1/2·7)
Interleukin 17	IL17	U32659	1/1·3	4·1	1/5·5 (1/8·0,1/3·7)
TBC1 domain family, member 15	TBC1D15	AK022147	1/2·0	2·2	1/4·5 (1/6·9, 1/2·9)
Syndecan 4 (amphiglycan, ryudocan)	SDC4	D13292	1·0	4·6	1/4·4 (1/5·2, 1/3·7)
Recombining binding protein suppressor of hairless (Drosophila)	RBPSUH	AW968632	1/2·3	1·7	1/4·0 (1/4·8, 1/3·3)
Humour necrosis factor, alpha-induced protein 6	TNFAIP6	M31165	5·5	22	1/3·9 (1/3·0, 1/5·2)
Hypothetical protein FLJ10199	FLJ10199	AI216532	1·0	3·8	1/3·9 (1/6·2, 1/2·4)
Small inducible cytokine subfamily B (Cys-X-Cys), member 11	CXCL11	AF030514	1·5	5·6	1/3·8 (1/2·7, 1/5·4)
Cathepsin L	CTSL	AI041851	5·5	21	1/3·8 (1/7·7, 1/1·9)
Enhancer of rudimentary homolog (Drosophila)	ERH	U66871	1/1·9	1·9	1/3·6 (1/3·0, 1/4·3)
Tryptophanyl-tRNA synthetase	WARS	X59892	1/1·7	2·1	1/3·6 (1/3·8, 1/3·4)
Epithelial membrane protein 1	EMP1	Y07909	1·2	4·4	1/3·6 (1/5·6, 1/2·3)
NADH dehydrogenase (ubiquinone) 1 alpha subcomplex, 5, 13 kDa	NDUFA5	U53468	1/3·7	1/1·1	1/3·4 (1/4·1, 1/2·9)
Hect domain and RLD 5	HERC5	AB027289	7·5	25	1/3·3 (1/1·2, 1/8·7)
Feline leukaemia virus subgroup C cellular receptor	FLVCR	AK001419	1/2·8	1·2	1/3·3 (1/5·2, 1/2·0)
FK506 binding protein 5	FKBP5	U42031	1/2·3	1·3	1/3·1 (1/4·5, 1/2·2)
Deleted in lymphocytic leukaemia, 2	DLEU2	AW978447	1/2·8	1·1	1/3·1 (1/2·1, 1/4·6)
Cathepsin L2	CTSL2	AB001928	4·2	13	1/3·0 (1/5·7, 1/1·6)
Methionine adenosyltransferase II, alpha	MAT2A	F07456	1/2·4	1·3	1/3·0 (1/1·8, 1/5·1)
v-maf musculoaponeurotic fibrosarcoma oncogene homolog (avian)	MAF	AF055376	1·0	2·9	1/3·0 (1/3·7, 1/2·5)

*Fold increase of the gene expression after stimulation with *Staphylococcus aureus*. **Fold difference of the change of the gene expression levels after stimulation with *Staphylococcus aureus* between two HIS patients and two healthy controls. Values in parentheses are the fold differences of the gene expression in each HIS patient compared with the mean expression value in healthy controls. Genes that showed more than 3 fold expressional differences between HIES and healthy controls were selected.

cytokine-related genes, the relative expression levels of *IL-17* and *small inducible cytokine subfamily B (Cys-X-Cys), member 11 (CXCL11)* genes after stimulation were decreased to 1/5·5 and 1/3·8, respectively, in HIES (Table 5). Analysis of the differences in functionally related gene groups in stimulated PBMNC from HIES patients and controls according to Gene Ontology Classifications revealed that a significantly larger number of immunoglobulin-related genes were up-regulated in HIES (29 of 1194 total up-regulated genes: 2·43%, $P < 0.05$ χ^2 test, Table 4).

These results showed unique patterns of the gene expression in unstimulated and stimulated conditions in peripheral blood cells from HIES patients.

Discussion

HIES is a multisystem disorder with the manifestations of recurrent infections especially with *Staphylococcus aureus*, characteristic facies, hyperextensibility of joints, multiple bone fractures, scoliosis, and delayed shedding of the primary teeth [4]. Therefore, it is likely that HIES is caused by a molecule which affects various biological functions rather than only by a Th1/Th2–related molecule. Chehimi *et al.* [8] analysed 375 cytokine and chemokine gene expression by microarray, and found that the expression of some chemokine genes was decreased in PBMNC of HIES after the stimulation with PHA, which may account for the decreased responsiveness against microorganisms. Because of the complex multisystem nature of this disease, we thought more comprehensive analysis of gene expression profiles in purified populations without and with the stimulation of *Staphylococcus aureus* would be necessary.

It is worthy of note that there were no remarkable differences in the whole gene expression levels of $CD4^+$ T cells containing Th1/Th2 cells between HIES patients and controls in an unstimulated condition. On the other hand, in unstimulated $CD14^+$ cells, 33 genes were up-regulated in HIES and unique gene expression patterns were observed in HIES (Tables 3 and 4). By quantitative PCR, the expression levels of *RGC32* that was the most up-regulated gene in microarray analysis, were significantly elevated in HIES compared with healthy controls and atopic dermatitis (Fig. 1). Although *RGC32* appears to be a cell cycle regulatory factor that mediates cell proliferation [13], it was not clear why the expression of *RGC32* was most up-regulated in $CD14^+$ cells in HIES and how it was related to the pathogenesis or pathophysiology of HIES. Nevertheless, the analysis of expression levels of *RGC32* would be helpful in the diagnosis of HIES. The down-regulation of a significantly large number of genes related to the cell growth and maintenance (Table 4) might contribute to the pathophysiology of HIES such as a decreased responsiveness against microorganisms.

After the stimulation with *Staphylococcus aureus*, decreased expression levels of *IL-17* and *CXCL11* genes were observed in PBMNC from patients with HIES (Table 5). IL-17, produced by T cells, is a proinflammatory cytokine that induces production of IL-1β and TNF-α by macrophages [14], and IL-6, IL-8 and GM-CSF by stromal cells [15]. It induces migration and functional maturation of neutrophils [16–18] and proinflammatory cytokine production by keratinocytes [19]. In addition, it is involved in the osteoclastogenesis [20]. *CXCL11* gene is located on chromosome 4q21, where HIES is linked. The chemokine, CXCL11 is produced by monocytes and keratinocytes after the stimulation with IFN-γ, and is also involved in the inflammatory response by inducing a chemotaxis of monocytes and activated T cells [21]. Osteoblasts express CXC chemokine receptor 3, the receptor of CXCL11 [22]. It is possible that a decreased expression of *IL-17* and *CXCL11* genes, of which translated products have pleiotropic biological activities, may play a role in the pathogenesis or pathophysiology of HIES.

One of the remarkable findings was up-regulation of immunoglobulin-related genes after the stimulation with *Staphylococcus aureus* (Table 4). It is reported that an increase of IgE levels was observed even in the cord blood of HIES [23], suggesting the primary dysregulation of IgE production. Our result suggested that the dysregulation was more generalized in immunoglobulin-related genes, and more prominent with the staphylococcal stimulation.

The number of patients used for the microarray analysis was low in this study, and it is possible that other genes or gene groups have more important meanings than those we picked up in the pathophysiology of HIES. Further genetic analysis based on the unique gene expression profile would clarify the pathophysiology and causative genetic abnormality of HIES, and help to develop a new diagnostic method in the near future.

Acknowledgements

We thank the following doctors for the cooperation in this study: Takefumi Matsuda, Department of Paediatrics, Japanese Red Cross Akita Hospital; Takeshi Ikegaya, Department of Paediatrics, Fujieda Municipal General Hospital; Kimio Minagawa, Department of Paediatrics, Hokkaido Children's Hospital and Medical Centre; Norio Onodera, Department of Paediatrics, Iwate Prefectural Hospital; Yoshihisa Nagatoshi, Department of Paediatrics, National Kyushu Cancer Centre; Satoru Yamaguchi, Department of Paediatrics, Fukuoka University; Koji Shinozaki, Department of Paediatrics, Sinshu University.

References

1 Davis SD, Schaller J, Wedgwood RJ. Job's syndrome: recurrent, 'cold', staphylococcal abscesses. Lancet 1966; 1:1013–5.

2 Buckley RH, Wray BB, Belmarker EZ. Extreme hyperimmunoglobulinemia E and undue susceptibility to infection. Pediatrics 1972; 49:59–70.

3 Hill HR, Ochs HD, Quie PG, Clark RA, Pabst HF, Klebanoff SJ, Wedgwood RJ. Defect in neutrophil granulocyte chemotaxis in

Job's syndrome of recurrent cold staphylococcal abscesses. Lancet 1974; **14**:617–9.

4 Grimbacher B, Holland SM, Gallin JI *et al.* Hyper–IgE syndrome with recurrent infections-an autosomal dominant multisystem disorder. N Engl J Med 1999; **340**:692–702.

5 Del Prete G, Tiri A, Maggi E *et al.* Defective in vitro production of γ-interferon and tumor necrosis factor-alpha by circulating T cells from patients with the hyper-immunoglobulin E syndrome. J Clin Invest 1989; **84**:1830–5.

6 Yokota S, Mitsuda T, Shimizu H, Ibe M, Ikezawa Z. Hyper IgE syndrome-a disease of imbalanced activation of helper T-cell subsets? Arerugi 1990; **39**:442–51.

7 Borges WG, Augustine NH, Hill HR. Defective interleukin-12/interferon-γ pathway in patients with hyperimmunoglobulinemia E syndrome. J Pediatr 2000; **136**:176–80.

8 Chehimi J, Elder M, Greene J, Noroski L, Stiehm ER, Winkelstein JA, Sullivan KE. Cytokine and chemokine dysregulation in hyper–IgE syndrome. Clin Immunol 2001; **100**:49–56.

9 Gudmundsson KO, Sigurjonsson OE, Gudmundsson S, Goldblatt D, Weemaes MR, Haraldsson A. Increased expression of interleukin-13 but not interleukin-4 in $CD4^+$ cells from patients with the hyper–IgE syndrome. Clin Exp Immunol 2002; **128**:532–7.

10 Vercelli D, Jabara HH, Cunningham-Rundles C, Abrams JS, Lewis DB, Meyer J, Schneider LC, Leung DY, Geha RS. Regulation of immunoglobulin (Ig) E synthesis in the hyper–IgE syndrome. J Clin Invest 1990; **85**:1666–71.

11 Rodriguez MF, Patino PJ, Montoya F, Montoya CJ, Sorensen RU. deOlarte DG. Interleukin 4 and interferon-γ secretion by antigen and mitogen stimulated mononuclear cells in the hyper–IgE syndrome: No TH-2 cytokine pattern. Ann Allergy Asthma Immunol 1998; **81**:443–7.

12 Grimbacher B, Schaffer AA, Holland SM *et al.* Genetic linkage of hyper–IgE syndrome to chromosome 4. Am J Hum Genet 1999; **65**:735–44.

13 Badea TC, Niculescu FI, Soane L, Shin ML, Rus H. Molecular cloning and characterization of RGC-32, a novel gene induced by complement activation in oligodendrocytes. J Biol Chem 1998; **41**:26977–81.

14 Jovanovic DV, Di Battista JA, Martel-Pelletier J, Jolicoeur FC, He Y, Zhang M. IL-17 stimulates the production and expression of proinflammatory cytokines, IL-1β and TNF-α, by human macrophages. J Immunol 1998; **160**:3513–21.

15 Fossiez F, Djossou O, Chomarat P *et al.* T-cell IL-17 induces stromal cells to produces proinflammatory and hematopoietic cytokines. J Exp Med 1996; **183**:2593–603.

16 Laan M, Cui ZH, Hoshino H, Lotvall J, Sjostrand M, Gruenert DC, Skoogh BE, Linden A. Neutrophil recruitment by human IL-17 via C-X-C chemokine release in the airways. J Immunol 1999; **162**:2347–52.

17 YeP, Rodriguez FH, Kanaly S *et al.* Recruitment of interleukin 17 receptor signaling for lung CXC chemokine and granulocyte colony-stimulating factor expression, neutrophil recruitment, and host defence. J Exp Med 2001; **194**:519–27.

18 Hoshino H, Laan M, Sjostrand M, Lotvall J, Skoogh BE, Linden A. Increased elastase and myeloperoxidase activity associated with neutrophil recruitment by IL-17 in airways in vivo. J Allergy Clin Immunol 2000; **105**:143–9.

19 Teunissen MB, Koomen CW, de Waal Malefyt R, Wierenga EA, Bos JD. Interleukin-17 and interferon-γ synergize in the enhancement of proinflammatory cytokine production by human keratinocytes. J Invest Dermatol 1998; **111**:645–9.

20 Kotake S, Udagawa N, Takahashi N *et al.* IL-17 in synovial fluids from patients with rheumatoid arthritis is a potent stimulator of osteoclastogenesis. J Clin Invest 1999; **103**:1345–52.

21 Cole KE, Strick CA, Paradis TJ *et al.* Interferon-inducible T cell alpha chemoattractant (I-TAC): a novel non-ELR CXC chemokine with potent activity on activated T cells through selective high affinity binding to CXCR3. J Exp Med 1998; **187**:2009–21.

22 Lisignoli G, Toneguzzi S, Piacentini A *et al.* Human osteoblasts express functional CXC chemokine receptors 3 and 5: Activation by their ligands, CXCL10 and CXCL13, significantly induces alkaline phosphatase and beta-N-acetylhexosaminidase release. J Cell Physiol 2003; **194**:71–9.

23 Dreskin SC, Gallin JI. Evolution of the hyperimmunoglobulin E and recurrent infection (HIE, Job's) syndrome in a young girl. J Allergy Clin Immunol 1987; **80**:746–51.

臨床免疫，44(1)：90-93，2005

話　題

IL-4/IL-13のダイオキシン類感受性への影響*

金地佐千子**　田中　剛**　出原賢治**

Key Words : dioxin, aryl hydrocarbon receptor, interleukin-4, microarray, IgE

はじめに

ダイオキシン(TCDD；2, 3, 7, 8-tetrachlorodibenzo-*p*-dioxin)は主にごみ焼却などの燃焼過程やクロロフェノールなどの農薬の製造過程で発生し，土壌，水質，大気汚染をひき起こすことが知られている．ダイオキシンはポリ塩化ジベンゾパラジオキシンの別称として用いられ，またポリ塩化ジベンゾフラン誘導体やコプラナPCB類も含めてダイオキシン類と総称される．ダイオキシン類は脂肪に蓄積しやすく，また代謝などによる排泄がされにくく，生体に対して皮膚毒性，発癌，生殖機能異常，免疫機能低下などの影響をもたらすことから社会的に大きな関心を呼んでいる．ダイオキシン類の免疫系への影響のひとつとしてアレルギー疾患の増悪へ関与する可能性も指摘されているが，いまだ解明が進んでいない．

ダイオキシンの作用機序

ダイオキシン類の生体への毒性の発現はAhR(aryl hydrocarbon receptor)を介して起こる．ダイオキシンは細胞内に入ると受容体であるAhRと結合し，活性化されたAhRは核へ移行する．核内でAhRはARNT(aryl hydrocarbon receptor nuclear translocator)という別の転写因子とヘテロダイマーを形成し，CYP1A1をはじめとする標的遺伝子のプロモーター領域に存在するXRE(xenobiotic responsive element)配列に結合して遺伝子発現を活性化する[1]．こうして誘導された薬物代謝酵素は外来異物の代謝を介した排出にかかわっている．AhR遺伝子欠損マウスではCYP1ファミリーの誘導は起こらず，またダイオキシン曝露による奇形や免疫抑制などの影響がみられないことからダイオキシンによる生体毒性の発現にはAhRが必須であることがわかっている[2]．

B細胞におけるIL-4/IL-13誘導遺伝子の同定

Th2サイトカインの中でIL-4/IL-13はB細胞におけるIgE産生を促進するなどアレルギー疾患の発症に重要な役割を果たすことが知られている．またIL-4/IL-13は免疫系細胞だけでなく気道上皮細胞や血管内皮細胞など非免疫系細胞に対しても多彩な生物活性をもつことが知られている．われわれはIL-4/IL-13の新規の生物活性の検索を行うため，マイクロアレイを用いてヒトバーキットリンパ腫由来B細胞株であるDND39におけるIL-4/IL-13誘導遺伝子の検索を行った．その結果得られた誘導遺伝子の中に，すでにIL-4/IL-13誘導遺伝子として知られているCD23，germline εなど以外にAhRが含まれていた[3]．ダイオキシン曝露によってマウスの胸腺萎縮が起こることなどからAhR活性化がT細胞に及ぼす影響についてはいくつかの検討がなされているが，B細胞におけるAhRの役割に関する知見は

* Effect of IL-4/IL-13 on the susceptibility to dioxin.

** Sachiko KANAJI, M.D., Ph.D., Go TANAKA, M.D., Ph.D. & Kenji IZUHARA, M.D., Ph.D.: 佐賀大学医学部分子生命科学講座分子医化学分野〔〒849-8501 佐賀市鍋島5-1-1〕; Division of Medical Biochemistry, Department of Biomolecular Sciences, Saga Medical School, Saga 849-8501, JAPAN